



UNIVERSITÀ DEGLI STUDI DI PADOVA

MSc in Environmental Engineering

ICEA Department

Master Thesis

Michele Rodighiero

**MODELLING BIO-HYDROGEN
PRODUCTION BY DARK FERMENTATION**

Supervisor

Prof. Ing. Raffaello Cossu

Co-supervisors

Dr. Ing. Luca Alibardi

Dr. Alessandro Spagni

Academic year

2014/2015

Acknowledgments

As I conclude my thesis, I would like to thank the people who have helped and supported me in invaluable ways during its realization and throughout my course of study.

It was a pleasure to have Alessandro Spagni and Luca Alibardi as co-supervisors and Annalisa Sandon as lab technician; capable, competent and caring individuals who supported and advised me like family both professionally and personally.

I thank my supervisor, Prof. Raffaello Cossu, for allowing me to join this research project.

Thanks to Luca Morello for having cheered up with his pleasantness my staying in the laboratory. Thanks to all the fellows I met during the past six months. I hope I will have the possibility to work with you again.

I would like to give especial thanks my girlfriend Elena for having been close to me, helping and supporting me during all these university years. I also thank my parents Loretta and Antonio and my brothers Francesco e Luca: I owe you much of what I am and have.

For all the opportunities and the unique values it instilled in me, I thank Collegio Universitario Don Nicola Mazza.

I would also like to mention and thank my friends of a lifetime and the more recent ones; sometimes a chat with the right people can change your day.

Contents

1	INTRODUCTION.....	10
1.1	Mathematical modelling of bio-hydrogen production by dark fermentation: state-of-the art	14
2	MATERIALS AND METHODS	17
2.1	Experimental set-up.....	17
2.1.1	Batch experiments	17
2.1.2	Continuous experiment	17
2.2	Inoculum and substrates	19
2.3	Analytical methods	19
3	MODEL DEVELOPMENT	20
3.1	Implementation on AQUASIM 2.1	26
3.1.1	Variables.....	26
3.1.2	Processes	29
3.1.3	Compartments	30
3.1.4	Sensitivity analysis and parameter estimation	32
4	RESULTS AND DISCUSSION	34
4.1	Sensitivity analysis	34
4.2	Model calibration.....	38
4.2.1	Model calibration on glucose BHP batch test	38
4.2.2	Model calibration on sucrose BHP batch test	42
4.2.3	Model calibration on mashed potatoes and potatoes peels BHP batch tests	45
4.2.4	Model calibration on wheat bran and durum wheat bran BHP batch tests	51
4.2.5	Model calibration on sucrose CSTR continuous test	57
5	CONCLUSIONS.....	62
6	REFERENCES.....	64

SECTION I:

My Thesis and Me

I began thinking about the topic of my Master thesis quite early, in winter 2013. During one of the last lectures of the Environmental Project Work course, Prof. Raffaello Cossu presented some research activities related to possible thesis works. When I heard about bio-hydrogen, I immediately set up my mind on that topic. I spoke with Dr. Luca Alibardi asking for more information about current and future projects in that area and we agreed to meet once back from my Erasmus experience in Denmark where, among other things, I would have followed a related course, *Bioenergy Technologies*. Therefore, in July 2014 I met Dr. Luca Alibardi and Dr. Alessandro Spagni who suggested me a particular topic, coupling biohydrogen generation and Dynamic Membrane technology. I knew very little about Membrane Bioreactors and even nothing about Dynamic Membranes technology applied to wastewater treatment but I was enthused and eager to start.

October 1st marked the beginning of my thesis work. I reached Dr. Luca Alibardi at the Voltabarozzo laboratory and he introduced me to the facility. Right away, he showed me the main components of my forthcoming system, the PVC pieces of the reactor, the membrane support and the effluent vessel. Almost all the material needed for the experimental set up was available or would be brought in the next days by Dr. Alessandro Spagni, therefore we were almost ready to start the construction phase. During the first two weeks, we prepared the lab-scale plant in every part, from assembling the steel shelving used as overall support and gluing the PVC pieces together (Figure 1). I spent a day threading the holes where the pipes holders would have been screwed while my co-supervisors prepared the main electrical components, i.e. timer for the effluent pump and level switch. I cut out from HDPE rolls the gasket of the reactor lids and the membrane support, assembled the U pipes used as pressure gauges and connected the digital display to the wet-tip gas meter.



Figure 1. My co-supervisors and me assembling the PVC parts of the experimental system. On the left with Dr. Luca Alibardi and the reactor, on the right with Dr. Alessandro Spagni and the effluent vessel.

During the second week, Marina Torrens Villorbina, bachelor student in Chemical Engineering from the University of Barcelona, arrived to the lab and began to work alongside me. In parallel to the assembling work, my co-supervisors, together with the technician Dr. Annalisa Sandon, taught me how to move in the chemistry lab and how to perform the periodical analysis. We also prepared the calibration curves to be set in the spectrophotometer for the determination of COD and total sugars concentration. Moreover, Nicoletta Bernava who was at the end of her path with a similar experimental system taught me how to manage the analysis schedule and other little tricks to ease the work.

At the end of the second week, we had the kickoff meeting, we talked about the feed composition and concentrations, the analysis to perform, the HRT and the pumping logic to use during the experiment. Of course, Marina and I were a little bit disoriented, incapable of suggesting options at the moment but Dr. Luca Alibardi and Dr. Alessandro Spagni were able to make us comfortable explaining the choices they were taking and sharing their expertise.

Finally, AnDy - the name of the setup, which stands for Anaerobic Dynamic membrane reactor - was ready for the startup. Figure 2 and 3 are pictures of me at work, preparing the sodium hydroxide solution for pH control and closing the reactor after the seed sludge inoculation, respectively.



Figure 3. Me diluting to the mark the sodium hydroxide solution for pH control



Figure 2. Me closing the reactor after the seed sludge inoculation

The first period was quite tiring but I knew that I just had to keep on going and I would have learned the analysis procedures, I would become able to recognize a proper result from a wrong one and I would have been more confident in managing the experimental setup. Of course, the more experience I acquired the more jaunty I felt in performing the “practical things” but it was not an easy path. We had several problems, especially within the first two months. Malfunctions of the experimental equipment coupled with the new tested conditions for the novel system slowed down the start-up and led us to several adjustments and decisions. Furthermore, being guided from distance, as my co-supervisors could not be physically present for the majority of the experimental trial, decelerated the decision-making.

Another inconvenient was that the gas chromatograph for volatile fatty acids analysis did not work during the experimental phase. It was, therefore, difficult to understand the biochemical processes that were going on in the fermenter. We kept filtered samples for future analysis in the freezer to trace back in a second moment what happened during the trial.

Even though no outstanding results were achieved, especially in the first period, during which we had to open the system several times, all the problems we had, allowed us to better understand the influence of the operating conditions and, in particular, on biomass requirements.

During the first month of trials we run the anaerobic membrane bioreactor not very successfully, we had continuous clogging of the membrane and leakages from the reactor. We decided to modify the membrane support thickness, change the recirculation peristaltic pump with a bigger one, increment the HRT from 1 to 4 days and increase the COD concentration in the feed from 10gL^{-1} to 50gL^{-1} . Moreover, we established to restart the system as a CSTR, thus without the filtration unit, to have a subsequently comparison with the performance of the membrane bioreactor.

At the end of November, we restarted the system as a CSTR (Figure 4). During this period, I started to use AQUASIM, a computer program for the identification and simulation of aquatic systems, to model our experimental setup. The idea was to develop a model, describing the dark fermentation process, applicable in both continuous and batch system. The model should represent a compromise between easy applicability and mechanistic description of the biochemical reactions. The CSTR run without particular problems for over a month; in the meanwhile, I worked on the modeling part. I researched in literature existing models and approaches and after a consultation with Dr. Alessandro Spagni, I decided to develop a model starting from the Anaerobic Digestion Model number 1 (ADM1) framework developed by the IWA task group. Therefore, in parallel with practical laboratory analysis and routine checks of the experimental system I wrote stoichiometric matrixes and elaborated a strategy to simulate dark fermentation with AQUASIM.

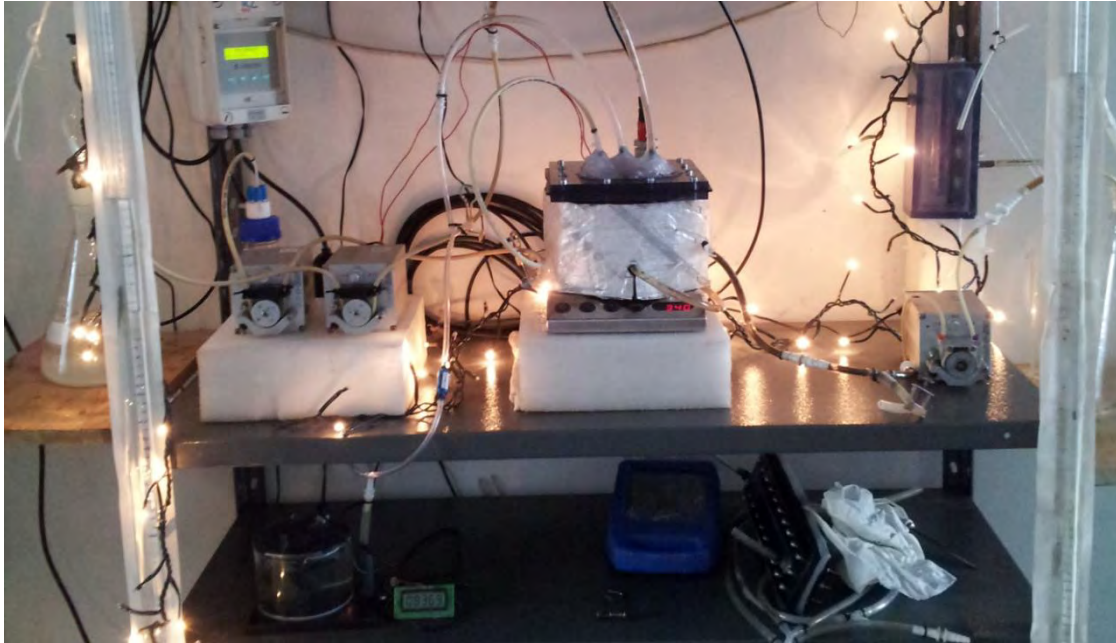


Figure 4. CSTR setup during the Christmas break

In the end of January, we revived the initial configuration adding the filtration module to the experimental setup. Unfortunately, the biomass concentration in the mix liquor was too low to allow the formation of a cake layer on the membrane nylon mesh, thus we had to re-inoculate. We took fresh anaerobic sludge, pretreated and seeded the reactor. At the same time, we performed BHP batch tests using the same inoculum of the reactor with three different substrate concentrations (Figure 5).



Figure 5. Bottles ready for the BHP test

We had an optimal startup of the AnMBR but after a week, the biogas production rate dropped down. There was a leak in the reactor, in correspondence of a pipe holder. We had to open the fermenter and seal the crack. Once fixed it, we closed again the reactor but in the next days, the hydrogen production remained very low. Probably some micronutrients, important for hydrogen fermentation were lacking in the feed. We tried to add some milk powder in the feed to see if it could provide some more nutrients but the attempt was in vain.

We understood that the thermally pretreated anaerobic sludge behave differently from the non-pretreated one in the presence of a membrane and that some micronutrients of secondary importance in anaerobic fermentation could be essential when fermenting hydrogen.

The time available for my thesis work was running out, so we decided to stop the experimental part of the study and to focus on the modeling work. The topic of my thesis was transferred to the model and I would have used all the applicable data retrieved during the experimental part for model simulations. Dr. Alessandro Spagni provided me some data coming from BHP batch tests on four carbohydrate rich industrial wastes. I used these data to calibrate the model, assess the variation of the model parameters and make a comparison between the simulations on different substrates. For the last two months, I worked with AQUASIM implementing the model, calibrating the parameters on various sets of data and simulating.

Overall, I enjoyed the six months spent for my thesis work. The problems we had with the experimental part and the subsequent decisions we took, enable me to have a more complete experience in the researching field. Not only I saw how to build and run a lab-scale anaerobic reactor and I learned how to perform several analysis, but I also understood an approach for modelling the dark fermentation process. I could take a close look to the research world, with its vicissitudes.

This experience was very formative and gave me the opportunity to meet and work side by side with nice, friendly, qualified and capable people.

SECTION II:

Scientific paper

1 INTRODUCTION

One of the great challenges going on worldwide, is the search for clean energy sources to mitigate coming climate change due to continuous emissions of greenhouse pollutants and the formation of CO_x , NO_x , SO_x , C_xH_y , ash, and other organic compounds that are released into the atmosphere as a result of combustion. Moreover, a shortage of readily available fuel to provide the energy required for present and future human activities is impending (Hallenbeck et al., 2012).

Until recently, almost all of the energy needed for heat and power generation, the industrial sector and the transportation, was derived from the conversion of non-renewable fossil energy sources (Das and Veziroğlu, 2001).

In the last decade, several studies has been conducted to obtain a sustainable, renewable source of energy that can gradually replace fossil fuels, fulfil the energy demand and which do not have a negative impact on the environment. Many authors proposed hydrogen as promising energy carrier to be used as alternative fuel. Hydrogen has an energy content of 122 kJ/g that is the highest among known gaseous fuels and is 2.75 times greater than hydrocarbon fuels (Argun et al., 2008). Besides being energy-efficient, H_2 is low-polluting; when it is used in a fuel cell to generate electricity or is combusted with air, the only products are water and a small amount of NO_x . Moreover, hydrogen gas is colourless, tasteless, odourless, light and non-toxic. It is considered a flexible, safe, affordable, domestic energy resource with a wide variety of applications, including fuel for vehicles, distributed and central electricity and thermal energy generation. However, so far more than 96% of H_2 is generated from fossil fuels and the largest users are the fertilizer and petroleum industries (Midilli et al., 2005; Meher Kotay and Das, 2008). A sustainable, renewable supply of hydrogen is therefore required and one option would be to use biological means such as direct- and indirect - photolysis, photo-fermentation, dark fermentation, or microbial electrolysis cells (MECs).

Direct photolysis is performed by cyanobacteria and green algae and it is associated with a photosynthesis process that uses sunlight to split water (Hallenbeck, 2011; Azwar et al., 2014). The merit of this process is that the principal feed is water, which is readily available and inexpensive. This process takes place under anaerobic conditions and currently requires a significant surface area to collect enough light. Alternatively, some algae can indirectly produce hydrogen under anaerobic, sulphur-deprivation condition; these algae in such a stressful environment, consume large amount of cellular starch and proteins to sustain indirectly the hydrogen production process (Show et al., 2012).

Photo-fermentation, carried out by purple bacteria, takes place in anoxic or anaerobic conditions and uses light as energy to convert organic compounds into hydrogen and CO₂ (Adessi and Philippis, 2012; Azwar et al., 2014; Show et al., 2012).

MECs for biohydrogen production through electro-hydrogenesis have been recently studied. This technology, also called bio-electrochemically assisted microbial reactor, is a type of modified microbial fuel cell, in which organic substrates are converted into biohydrogen under a supply of external voltage (Show et al., 2011).

Finally, another possibility is dark fermentation (DF) or heterotrophic fermentation in which organic compounds are converted to biohydrogen by diverse groups of bacteria through a series of biochemical reactions under anaerobic conditions.

Among the listed possibilities, DF seems to be more favourable, since hydrogen is yielded at a high rate and low cost when using various organic substrates, particularly with renewable resources that are rich in organic matter such as stillage, sludge, leachate, pomace, stalks, bagasse, waste and wastewaters. Moreover it has the ability of continuous hydrogen production without an external energy supply or a light source and can simultaneously solve problems of waste disposal with the utilization of human-derived organic wastes.

Microorganisms derive electrons from the oxidation of energy-rich molecules to drive energy generation. In the absence of external electron acceptors, hydrogen-producing bacteria dispose the excess of electrons generated during metabolism by reducing protons to hydrogen. In the fermentation pathways leading to hydrogen from glycolytic breakdown of carbohydrate-derived sugars, pyruvate is the key intermediate (Hallenbeck, 2009). In fact, monosaccharides are first converted by hydrogen producing bacteria (HPB) to pyruvate, generating the reduced form of nicotinamide adenine dinucleotide (NADH). Pyruvate is then further converted to acetyl-CoA and formate, which may be readily converted to hydrogen and carbon dioxide. Acetyl-CoA is finally transformed into some soluble metabolites such as acetate, butyrate, ethanol and others (Wang and Wan, 2009).

Actually, fermentative hydrogen production is a very complex process and is influenced by many factors such as inoculum, substrate, macro- and micronutrients (i.e. nitrogen, phosphate and metal ions), temperature, pH, reactor type and configuration.

Biohydrogen production by DF can be carried out by pure or mixed cultures. However, the use of pure cultures is expensive and technically difficult since it requires sterile conditions and strict control of environmental conditions. Most of the studies using pure cultures were conducted in batch mode and using simple substrate such as glucose. Mixed cultures, on the contrary, offer many advantages, such as easy control of the process and high stability in the H₂ production rate, leading,

therefore, to a preference in large-scale processes where continuous hydrogen production is required. Moreover, seed sludge containing a diverse microflora can use a broad source of feedstock and can adapt to environmental stresses including limited substrates, changes in pH and temperature variations (de Sá et al., 2013; Wang and Wan, 2009; Wong et al., 2014). Bacteria capable of producing hydrogen widely exist in natural environments such as soil, wastewater sludge, anaerobic sludge and compost. However, the microflora presents in the seed sludge usually consists of both HPB and H₂-consuming bacteria (HCB). As a result, hydrogen usually does not accumulate in the environment. Therefore, in order to minimize the presence of HCB and enhance the net hydrogen production, the inoculum is pre-treated using various physical (heat, aeration, ultraviolet, ultrasonic, freezing/thawing) and chemical (acid, alkali or organic compounds) methods. The determination of the most effective pre-treatment method is still under investigation and it may not be univocal since the optimal procedure for enriching HPB depends on the type of inoculum, the specific condition and the kind of substrate. However, the spore-forming enrichment by heat treatment is the most common, although temperature and time of application vary significantly (Hawkes et al., 2007).

Several substrates have been tested for fermentative hydrogen production, from glucose, sucrose, soluble and particulate starch and cellulose to rice slurry, beer lees, food waste and wastewater. However, from recent studies it seems that organic substrates mainly composed of either proteins or lipids are not suitable for hydrogen production via dark fermentation (Alibardi and Cossu, 2015; Boni et al., 2013). In fact, amino acids produced from the hydrolysis of proteins are fermented yielding no hydrogen while long chain fatty acids (LCFAs) from lipids hydrolysis can be converted to acetate and hydrogen only at extremely low partial pressure of hydrogen (Hallenbeck, 2009). The most appropriate substrate are those rich in sugars such as agricultural or food industry wastes containing starch and cellulose and industrial wastewaters from dairy industry and breweries (Kapdan and Kargi, 2006).

The production of H₂ from carbohydrate-rich complex materials has been studied mainly in batch conditions because of the difficulty of delivering particulate matter to continuous reactor at laboratory scale. It has been shown that in an appropriate range, increasing substrate concentration could increase the ability of HPB to produce hydrogen during fermentation but exist a certain disagreement on the optimal values, probably because of the differences in terms of inoculum and range of concentrations considered (Lo et al., 2008; Van Ginkel and Logan, 2005).

The macronutrients in DF, besides carbon (C), are nitrogen (N) and phosphorous (P) that are usually present as ammonium and phosphate respectively. A balanced nutrient level is essential for optimum H₂ production. Metal ions are instead micronutrients for fermentation; Nickel (Ni)

and iron (Fe), for example, serve as co-factors for the hydrogenase, the main enzyme responsible for H₂ generation (Hawkes et al., 2007; Wong et al., 2014).

Temperature is an important factor, influencing the activities of HPB. Most of the studies has been conducted in the mesophilic range (20-45°C) because the majority of the seeds were mesophilic sludge.

pH plays a critical role in sustaining the growth of HPB and the activity of hydrogenase in H₂ production. The metabolic pathways yielding higher hydrogen generation, i.e. involving acetate and butyrate production, appear to be favoured at pH range 4.5-6. At pH lower than 4.5 a shift from acidogenesis to solvent production has been observed because of the build up of VFAs and H₂. Hence, a stable pH is essential to sustain optimum hydrogen production (De Gioannis et al., 2013).

The design and the operating conditions of bioreactors are crucial elements for continuous dark fermentative hydrogen production. At laboratory scale, continuous stirred tank reactors (CSTRs) are the most common systems (Hawkes et al., 2007; Show et al., 2011). This configuration has been widely investigated as it allows researchers to obtain operating parameters in various conditions. Complete mixing allows intimate contact between substrate and biomass, as well as effective pH and temperature control.

The use of dark fermentative processes for waste treatment presents many drawbacks since it does not stabilise the substrate but leads to a mix of VFAs and alcohols as final products. Therefore, it is necessary a further downstream process of these metabolites to recover either valuable products or additional energy. Possible downstream processes for energy recovery include photo-fermentation to produce additional hydrogen (Chen et al., 2008), microbial fuel cell or microbial electrolysis cells to produce electricity (Lalauette et al., 2009; Oh and Logan, 2005) and anaerobic digestion to produce methane (Liu et al., 2006).

In designing such two-stage processes, it would be desirable to be able to predict the end products of DF. This ability can be beneficial not only in optimising the design, operation, and scale up of the DF process itself, but also in selecting and designing appropriate downstream treatments, and in optimising the integrated process.

The use of mathematical models can help the understanding of the processes taking place and can improve reactor design. Moreover, mathematical models enable the forecasting of the behaviour of the state variables and the effect of varying operating conditions.

Models, thus, can be beneficial in designing experiments for testing, refining, and validating hypotheses and for in-depth analysis of the processes that may not be possible to realise experimentally (Argun et al., 2008; Rasika J. Perera and Nirmalakhandan, 2011).

1.1 Mathematical modelling of bio-hydrogen production by dark fermentation: state-of-the art

Several modelling methods have been developed with the purpose of improving, analysing and predicting biohydrogen production. The existing models could be divided into two main categories: kinetic models and experimental design methods. The first are applied to predict microbial growth, product formation and degradation of organic substrate during fermentative hydrogen production; the second are used to investigate the effects of physico-chemical parameters for process optimization (Nath and Das, 2011).

In the past decade, several experimental studies have been reported on dark fermentation of pure organic substrates, complex organic liquid wastes, and complex particulate substrates (Arudchelvam et al., 2010). Many of the studies on pure substrates had adapted the Gompertz equation or a modified form of it to fit the experimentally measured hydrogen evolution data (Mu et al., 2007, Gadhamshetty et al., 2010 and Chen et al., 2006). Others had adapted well-known models such as the Monod model (Chen et al., 2006; Lin et al., 2006; Lo et al., 2008) to describe the kinetics of bacterial growth and hydrogen production. Some authors started from models as Andrew model (Wang and Wan, 2008 and Zheng et al., 2008), Arrhenius model (Mu et al., 2006 and Lin et al., 2006), Luedeking–Piret model and the modified Luedeking–Piret model (Lo et al., 2008; Mu et al., 2006) to describe the fermentative hydrogen evolution.

What emerges from these approaches is that they are not able to represent the overall dark fermentative process, but they rather describe parts of it. In addition, models such as the Luedeking–Piret model and the modified Gompertz equation use coefficients that have little value from a biochemical point of view. In the former, for example, to describe the relationship between biomass and products are used a growth-associated formation coefficient and a non-growth-associated formation coefficient of product *i*-th. The estimation of these two values gives worthless, too general information about the metabolism of the hydrogen-producing biomass. In the modified Gompertz equation the formation kinetics of products are not directly related to the substrate or to the biomass, but are modelled using coefficients representing a general maximum rate of product formed and a lag time.

Other approaches are to use pseudo-stoichiometric dynamic models, as the one used by Aceves-Lara et al. (2008) to describe hydrogen production from molasses. Even if the latter models are able to describe more completely the fermentation process, the risk with pure pseudo-

stoichiometric matrixes is to lose the mechanistic description of the biochemical reactions obtaining the parameters from a mere mathematical fitting.

Recently, more complex models have been used by researchers, such as modified versions of the IWA Anaerobic Digestion Model n.1 (ADM1). This model was developed for describing the anaerobic digestion process and has widely been applied. The ADM1 includes the major processes involved in the bioconversion of complex organic substrates into methane, carbon dioxide and inert by products with the metabolic intermediates being mainly VFAs. The application of the model to non-methanogenic systems demands modifications, since the initial model structure uses constant stoichiometry to describe product generation from carbohydrates fermentation as well as it does not account for lactic acid and ethanol production that are important metabolites in non-methanogenic processes. The ADM1 framework with appropriate changes has been used for describing the performance of both pure and mixed cultures in either batch or continuous dark fermentation systems.

A modified version of the ADM1 has been used by Lin et al. (2007) to simulate clostridial glucose fermentation process in batch cultures. Ntaikou et al. (2010) developed and applied a version of ADM1 to describe and predict batch and continuous fermentative hydrogen production by the bacterium *Ruminococcus albus*. Rodríguez et al. (2006) proposed a variable stoichiometry function integrated to ADM1 in order to describe the products formation. Penumathsa et al. (2008) used a modified version of the model to predict the production of VFA and hydrogen with sucrose as substrate using a variable stoichiometry approach derived from experimental information.

Gadhamshetty et al. (2010) and Arudchelvam et al. (2010) presented a model, derived from the assumption of ADM1 for predicting VFAs formation from sucrose and from particulate substrates respectively.

Of course, this kind of models describe more completely the dark fermentation process but bring an incremental complexity, which leads to an increasing uncertainty. The use of complicated models to have a rapid assessment of the processes and the data acquired along an experimental phase is not thrilling. Initial conditions and input data of the state variables are needed and the calibration step may require to estimate several process parameters (hydrolysis parameters, biouptake parameters, yield factors) the number of which increase with the increasing model complexity.

That is why the majority of the researchers have used simple models, as the modified Gompertz equation to describe their experimental data as the hydrogen evolution in batch tests. However, this equation cannot be applied in continuous systems and cannot predict concentration of substrates utilized and metabolites produced along with hydrogen (Antonopoulou et al., 2012).

Moreover, a model should be based on appropriate kinetic parameters, describing the biochemical activity of the biomass. This would enable comparisons with other kinetics models and lead to increase understanding of the process. What should be sought is a compromise between simplicity of application and biochemical meaning, maintaining thus the model simple while describing mechanistically the processes involved.

The aim of this study is to investigate the applicability of a derived ADM1 model, with a low degree of complexity, for the description of hydrogen production, metabolites generation and substrate utilization in batch and continuous systems using mixed microbial cultures and carbohydrates rich substrates. The kinetic parameters for substrate consumption and the yield coefficients of VFAs, hydrogen and solvents production were estimated using experiments and by literature data obtained by Giordano et al. (2011). The developed model was applied to batch experiments with different substrates. Moreover, a bench-scale CSTR fed with sucrose was run for over a month to assess the model predictions in continuous hydrogen production.

2 MATERIALS AND METHODS

The data utilised in the development of the present model, were obtained from two different sources. The first source is the experimental activity with sucrose as substrate that was conducted during this study, consisting in batch tests and a continuous test using a CSTR configuration. The rest of the data, coming from batch tests for assessing the biochemical hydrogen potential of wheat bran of *Triticum durum*, wheat bran of *Triticum aestivum*, wastes from steam-peeling potato-processing and wastes of the industrial production of mashed potatoes, were obtained from literature (Giordano et al., 2011). For the experimental set-up and the analytic methods used to collect the literature data, the reader should refer to Giordano et al. (2011).

2.1 Experimental set-up

2.1.1 Batch experiments

Laboratory-scale experiments were performed to evaluate the Biochemical Hydrogen Potential (BHP) of sucrose in three different ratios between the volatile solids of the substrate to be degraded and volatile solids of the inoculum biomass (F/M). Tests were carried out in 0.5 L batch reactors under mesophilic conditions (35 ± 1 °C). Reactors were airtight closed by means of a silicon plug enabling sampling of the gas produced during fermentation. The liquid volume in each reactor, consisting of the substrate, inoculum and tap water, was 250 ml. Tests were performed at a substrate concentration of 2.08, 1.04 and 0.52 g_{VS}L⁻¹. The F/M was 2, 1 and 0.5 g_{VS}/g_{VS} respectively. Heat pre-treated anaerobic sludge was used as inoculum.

After preparation, the reactors were flushed with N₂ for 3 min in order to remove the atmospheric air. Thereafter, the reactors were incubated under static conditions in a thermostatic chamber. Blank tests using the inoculum alone were also prepared to measure the quantity of hydrogen produced by the biomass only. All tests were carried out in triplicate.

Data on hydrogen productions are expressed at a temperature of 20°C and pressure of 1 atm (NTP).

2.1.2 Continuous experiment

The CSTR had a total volume of 1 L (W x H x D: 10 x 10 x 10 cm) and a working volume of 775 mL. The mixed liquor level was maintained constant by a level sensor directly connected to the influent peristaltic pump (Watson Marlow 401U/D1, Falmouth, Cornwall, UK).

The effluent was controlled by a second peristaltic pump (Watson Marlow 401U/DM3, Falmouth, Cornwall, UK). It was collected in a vessel and analysed approximately three times per week.

The biogas production was monitored by using a homemade wet-tip gas meters; directly connected on the anaerobic reactor (Figure 6).

The reactor was operated continuously at mesophilic temperature of $35\pm 1^\circ\text{C}$ maintained by a thermostatic bath (IS Co. GTR 2000 “11x”, Italy). Mixing was carried out using a magnetic stirrer (Variomag Maxi Direct, Thermo Scientific, Italy). pH was maintained at 5.0 ± 0.1 using a pH controller (Crison 28 carrying a pH probe Crison 53 35) connected to a peristaltic pump (Watson Marlow 401U/D1, Falmouth, Cornwall, UK) dosing NaOH 2.5 M.

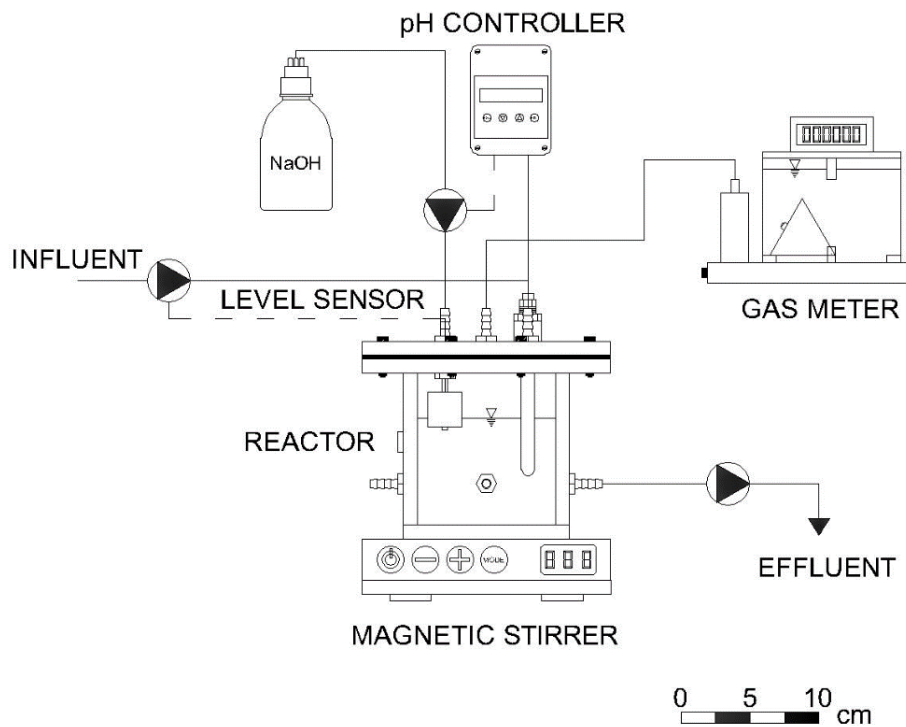


Figure 6. Schematic diagram of the experimental setup. Reactor and wet-tip gas-meter are drawn to scale.

To start-up the system, the reactor was filled with 0.6 L of heat pre-treated, screened, anaerobic sludge and 0.2 L of feed solution. The feed concentration was kept constant except between day 18 and 27 when it was halved. On the contrary, the HRT was maintained around 4 days along all the 40 days period. The changing in feed concentration induced a variation in the daily averaged organic loading rate (OLR) from $12.5 \text{ gCOD L}^{-1} \text{ d}^{-1}$ to $6.25 \text{ gCOD L}^{-1} \text{ d}^{-1}$.

2.2 Inoculum and substrates

The CSTR was seeded with anaerobic sludge obtained from a full-scale mesophilic anaerobic digester treating the excess sludge of the municipal wastewater treatment plant of Ca' Nordio (Padova, Italy). The sludge was pretreated at 80°C for 30 min before inoculation in order to select for hydrogen producing biomass. The main characteristics of the seed sludge were as follow: pH = 7.5; total solids (TS, g/L) = 11.2; volatile solids (VS, g/L) = 5.2.

The reactor was fed with synthetic wastewater containing sucrose as the only carbon source at a concentration of 25 and 50 g_{COD} L⁻¹. The followings chemicals were added in order to assure the presence of buffers, nutrients and microelements: NaHCO₃ (1660 mg L⁻¹_{feed}), NH₄Cl (100 mgN L⁻¹_{feed}), KH₂PO₄ (10 mgP L⁻¹_{feed}), FeCl₃·6H₂O (2.1 mgFe L⁻¹_{feed}), CaCl₂·2H₂O (8.2 mgCa L⁻¹_{feed}), MgCl₂·6H₂O (2.4 mgMg L⁻¹_{feed}), Na₂MoO₄·2H₂O (0.22 mgMo L⁻¹_{feed}), ZnSO₄·7H₂O (0.23 mgZn L⁻¹_{feed}), CuSO₄·5H₂O (0.128 mgCu L⁻¹_{feed}), NiCl₂·6H₂O (0.1 mgNi L⁻¹_{feed}), H₃BO₄ (0.007 mgB L⁻¹_{feed}). All the compounds were dissolved in tap water. The feed solution utilized in the continuous experiment was the same prepared for the BHP tests with different concentration of sucrose.

2.3 Analytical methods

To evaluate the performance of the CSTR system, periodical analysis on the effluent and biogas were performed. On the effluent, the following parameters were analysed: total COD, filterable COD, soluble COD, total (TSS) and volatile suspended solids (VSS), pH, alkalinity, NH₄⁺, total P and dissolved P concentration. To determine soluble COD, and for the VFAs analysis, the samples were first centrifuged at 6000 rpm for 15 minutes and then filtered using 0.2 µm syringe filters (PTFE, 25mm – 0.2 µm). COD, TSS, VSS, pH, alkalinity, NH₄⁺-N, total P and dissolved P concentration were measured according to Standard Methods (APHA, 2005). Whatman GF/C filters were used for TSS and VSS measurements. Sucrose was measured according to Dubois et al. (1956).

Biogas composition was measured by a micro-gas chromatograph (Varian 490-GC) equipped with a 10 m MS5A column and 10 m PPU column, using argon as carrier gas and a thermal conductivity detector. Volatile fatty acids (VFAs, acetic, propionic, butyric acids) were measured by a gas chromatograph (Varian 3800) equipped with a flame ionization detector, a 25m × 0.53mm × 0.70mm CP-Wax 58 (FFAP) CB capillary column (Varian) and using nitrogen as carrier gas.

The biogas volume produced during BHP tests with sucrose was measured at room temperature by means of the water displacement method. Biogas quality was analysed through a micro-gas chromatograph (Varian 490-GC) equipped with a 10 m MS5A column and 10 m PPU column, using argon as carrier gas and a thermal conductivity detector.

3 MODEL DEVELOPMENT

In this study, the ADM1 has been used as a basis for the definition of variables and processes. The basic structure of the model was modified in order to make it more reliable for describing the biohydrogen production process from carbohydrate-rich substrates. Firstly, the methanogenic step was switched off and, thus, the acidogenic phase only was considered. Methanogens and acetogens were not considered in the model since no methane was detected at all in the experimental phases and because the high hydrogen partial pressure is prohibitive for the growth of propionate, butyrate and long chain fatty acids degraders.

As was already mentioned in the introductory chapter, fermentation of proteins and lipids does not yield hydrogen. Therefore, it is pointless to model it in the specific, especially when the focus is on carbohydrate rich substrates. In the present model, the biochemical pathways yielding hydrogen and VFAs come from the metabolization of sugars, but thanks to the variable stoichiometry introduced, it is possible to generalize the application. Acidogenesis of carbohydrates is known to simultaneously produce hydrogen, carbon dioxide, VFAs and, depending on the operating conditions, lactate and alcohols. These, last mentioned, reduced end-products, such as ethanol, butanol and lactate, contain additional H atoms that are not liberated as gas and are therefore lowering the yield of hydrogen. They are considered in the model under the general nomenclature of solvents. The biochemical reactions were written considering a COD mass balance and, therefore, all organic substances and molecular hydrogen were described in terms of chemical oxygen demand ($\text{g}_{\text{COD}} \text{L}^{-1}$). Since substrates can be characterised as inert materials under hydrogen producing conditions, the proposed model assumes that only a fraction of the input COD of a complex feedstock is disintegrated, hydrolysed and subsequently utilised by the acidogenic biomass. Therefore, a factor (f_{bio}) standing for the biodegradable fraction of the input COD was introduced (Table 3-1). Complex particulate substrate is assumed homogeneous. The initial substrate is disintegrated into an inert fraction and a biodegradable fraction under fermentative conditions following a first order kinetic (1).

$$\frac{dX_{sub}}{dt} = -k_{dis} X_{sub} \quad (1)$$

where k_{dis} is the disintegration kinetic parameter expressed as d^{-1} and X_{sub} is the concentration of substrate ($\text{g}_{\text{COD}} \text{L}^{-1}$).

The biodegradable fraction is then hydrolysed into its monomers. Proteins and lipids present in the substrate are not directly considered in the model, being that they do not contribute to hydrogen

production. The modelled bacterial metabolism relies mainly on carbohydrate, therefore this fraction will be explicitly described. Metabolites, substrate consumption and biomass growth dependent on proteins or lipids are implicitly accounted in the model.

Once the particulate fermentable substrate have been solubilized through the hydrolytic step, it is converted into biomass, VFAs (acetic, propionic and butyric acid), hydrogen and solvents (that close the mass balance and comprehend mainly alcohols). As mentioned before, since the model solves a COD mass balance, carbon dioxide production is not accounted.

Hydrolysis is described by a surface limiting rate expression; therefore, the rate of change of particulate concentration of fermentable substrate can be described by:

$$\frac{dS_f}{dt} = -k_{hyd} \left(\frac{S_f/X_B}{K_x + S_f/X_B} \right) X_B \quad (2)$$

where k_{hyd} is the rate constant (d^{-1}), K_x is the saturation coefficient for hydrolysis, S_f is the concentration of substrate ($g_{COD}L^{-1}$) and X_B the concentration of the biomass ($g_{COD}L^{-1}$).

The following uptake rate of hydrolysed substrate (in the present study, mainly monosaccharides and the soluble forms of cellulose and hemicellulose) by acidogens is modelled using a single-substrate-single biomass expression based on an uninhibited Monod-type kinetic:

$$\frac{dS_f}{dt} = -k_m \frac{S_f}{K_f + S_f} X_B \quad (3)$$

where k_m is the Monod maximum specific uptake rate ($g_{COD_S} g_{COD_X}^{-1} d^{-1}$), K_s is the half saturation constant ($g_{COD}L^{-1}$) and S_f is the concentration of fermentable hydrolysed substrate ($g_{COD}L^{-1}$).

Rate of growth of biomass is considered proportional to the uptake rate of S_f with the appropriate yield coefficient (Y_B). The net rate of change of biomass (X_B) is then obtained by including the decay rate:

$$\frac{dX_B}{dt} = -\frac{dS_f}{dt} Y_B - X_B b \quad (4)$$

From the biomass decay process, three particulate fractions are obtained (Table 3-2): f_f , which is fermentable, f_s that is organic but not fermentable and $(1 - f_f - f_s)$ representing the inert fraction.

Moreover, the rate of product formation consider that a fraction of the up-taken COD is utilized for VFAs, hydrogen and “other” formation. The term “other” englobes solvents and other metabolic products, such as lactate, that close the COD mass balance of the model. In fact, the sugar fermentation pathway can result in a number of products apart from organic acids, the most important of which are lactate and ethanol in anaerobic digesters (Antonopoulou et al., 2012).

It was assumed that further degradation of VFAs does not take place under the tested conditions and that the hydrogen produced is not consumed by any reaction. The following equation describes the rate of formation of the product i ($i=ac$ for acetic acid, $i=pro$ for propionic acid, $i=bu$ for butyric acid, $i=h_2$ for hydrogen, $i=others$ for solvents and others) from the uptake of the hydrolysed fermentable substrate:

$$\frac{dS_i}{dt} = -\frac{dS_f}{dt} (1 - Y_B) f_i \quad (5)$$

where f_i represent the stoichiometric coefficients ($g_{COD} g_{COD}^{-1}$) of the products formation. In the ADM1, the product yield coefficient f_i is actually the parameter describing the distribution of metabolites, since it expresses the ratio of COD that is catabolized to a certain product from the overall net COD that is catabolized to products, without taking into consideration the amount of carbon incorporated in the biomass.

The ratios of products from monosaccharide fermentation such as acetate, propionate and butyrate can be simplified by assuming that fermentation proceeds by three key reactions as presented in Table 3-1 (Batstone et al., 2002) where glucose is assumed as representative sugar monolith. The fraction of monosaccharide degraded via the first, second and third reaction can be expressed as $n_{1,mo}$, $n_{2,mo}$ and $n_{3,mo}$ respectively. In the ADM1 the sum of the aforementioned coefficients is set equal to one (6) being that lactate end ethanol, as well as other solvents are excluded from the model. Based on ADM1:

$$1 - n_{1,mo} - n_{2,mo} = n_{3,mo} \quad (6)$$

According to the present model assumptions and to previous works present in literature (Antonopoulou et al., 2012; Penumathsa et al., 2008), to take into consideration the production of metabolites other than acetic, propionic and butyric acid, the above expression (6) was modified so that the sum of the glucose fractions is different from the unit. For this porpoise a dimensionless

coefficient, representing the rate of acidogenesis (r_{acid}) ranging from zero (no VFAs formation) to one (complete conversion of monosaccharides to VFAs) was introduced. It multiplies the coefficients $n_{1,mo}$, $n_{2,mo}$ and $n_{3,mo}$ when calculating the product yields (7)-(10). Moreover, in order to have a variable stoichiometry, other two coefficients have been introduced in the calculation of the product yields ($h_{2,ac}$ and $h_{2,bu}$). These two coefficients represent the moles of hydrogen formed per mole of $C_6H_{12}O_2$ through acetic acid ($h_{2,ac}$) and butyric acid ($h_{2,bu}$) fermentation, respectively. The relatively lower yield of hydrogen during fermentation is a natural consequence of the fact that fermentations have been optimized by evolution to produce cell biomass and not hydrogen (Nath and Das, 2004). Moreover, in many organisms the actual yields of hydrogen are reduced by hydrogen recycling owing to the presence of one or more uptake hydrogenases, which consume a part of the produced hydrogen (Hallenbeck and Benemann, 2002). From a thermodynamic perspective, the most favourable products from the breakdown of 1 mol glucose are the 2 mol acetates and 4 mol H_2 shown in Table 3-1. However, this stoichiometric yield is only attainable under near-equilibrium conditions, which implies very slow rates and/or at very low hydrogen partial pressures (Hallenbeck and Benemann, 2002).

Table 3-1. Monosaccharide equations and stoichiometric coefficients implemented in ADM1

Reactions of glucose degradation in ADM1	Glucose fractions	Products of glucose degradation	Stoichiometric coefficients, gCOD/gCOD
$C_6H_{12}O_6 + 2H_2O \rightarrow 2CH_3COOH + 2CO_2 + 4H_2$	$n_{1,mo}$	Acetic acid	$f_{ac,mo} = 0.67 n_{1,mo} + 0.22 n_{2,mo}$
$3C_6H_{12}O_6 \rightarrow 4CH_3CH_2COOH + 2CH_3COOH + 2CO_2 + 2H_2O$	$n_{2,mo}$	Propionic acid	$f_{pro,mo} = 0.78 n_{2,mo}$
$C_6H_{12}O_6 \rightarrow CH_3CH_2CH_2COOH + 2CO_2 + 2H_2$	$n_{3,mo}$	Butyric acid	$f_{bu,mo} = 0.83 n_{3,mo}$
		Hydrogen	$f_{h2,mo} = 0.33 n_{1,mo} + 0.17 n_{3,mo}$

In ADM1, as can be seen in Table 3-1, considering the first of the three reactions, from one mole of monosaccharide, equal to 192 gCOD (see Table 3-3), four moles of hydrogen (64 gCOD) and two moles of acetic acid (128 gCOD) are obtained. Therefore, one third (0.33) of the initial COD is converted into hydrogen. This fraction is set as the upper limit of $h_{2,ac}$. When $h_{2,ac}$ is lower than 0.33, the fraction of sugar converted into hydrogen diminish while more acid is produced. Thus, the yield of H_2 in the acetic acid pathway is lowered.

The third reaction results into two moles of hydrogen (32 gCOD) and one mole of butyric acid (160 gCOD) per mole of monosaccharide (192gCOD). The fraction of the COD passed to hydrogen is one sixth (0.17), value set as upper limit for $h_{2,bu}$. Of course, $(1-h_{2,bu})$ represent the fraction of initial COD transformed into butyric acid through the butyrate reaction path.

From the second reaction in Table 3-1 only acids are produced. From 192 gCOD as monosaccharide, 149.76 gCOD as propionate and 42.24 gCOD as acetate are produced.

Once marked the three main fermentative reactions with $n_{1,mo}$, $n_{2,mo}$ and $n_{3,mo}$, introduced the fraction r_{acid} of monosaccharides that are diverted into the three pathways and adjusted the fate of COD within the reactions through $h_{2,ac}$ and $h_{2,bu}$ the overall product yields can be calculated.

The stoichiometric coefficients, or product yields, represent the fractions of initial soluble fermentative substrate used for the bacterial catabolism, which are diverted in the different catabolic pathways. They were determined from the model using the following equations (7)-(10):

$$f_{ac} = \left((1 - h_{2,ac}) n_{1,mo} + 0.22 n_{2,mo} \right) r_{acid} \quad (7)$$

$$f_{pro} = (0.78 n_{2,mo}) r_{acid} \quad (8)$$

$$f_{bu} = \left((1 - h_{2,bu}) n_{3,mo} \right) r_{acid} \quad (9)$$

$$f_{h2} = (h_{2,ac} n_{1,mo} + h_{2,bu} n_{3,mo}) r_{acid} \quad (10)$$

The fractions $n_{1,mo}$ and $n_{2,mo}$, as well as r_{acid} were estimated using the experimental data in relation to the concentrations of produced VFAs, whereas the yields $h_{2,ac}$ and $h_{2,bu}$ were calibrated on the observed hydrogen production.

To close the mass balance was used the generation of solvents and lactate, so the fraction of their formation is defined as:

$$f_{others} = 1 - (f_{ac} + f_{pro} + f_{bu} + f_{h2}) \quad (11)$$

An overall view of the biological kinetic rate expressions and coefficients is shown in Peterson matrix form in Table 3-2. As previously stated, the hydrogen generated during the bacterial metabolism is assumed to be directly present in its gaseous form, neglecting the diffusion process. The concentration in $g_{COD}L^{-1}$ of H_2 is thus multiplied to the liquid volume of the reactor; the mass is expressed as moles and then transformed into liters at room temperature (12).

$$H_2(L) = S_{h2} (g_{COD}L^{-1}) V_{reactor}(L) \frac{1}{16} (mol g_{COD}^{-1}) 24 (L_{gas}mol^{-1}) \quad (12)$$

In the case of the CSTR configuration, to get the hydrogen production rate in Ld^{-1} , the above expression is simply multiplied to the hydraulic retention time

Table 3-2. Biochemical rate coefficients and kinetic rate equations

j	i	Component → Process ↓	X_{sub}	X_f	S_f	S_{ac}	S_{pro}	S_{bu}	H_2	S_{others}	X_B	X_s	X_i	Rate	
1		Disintegration of X_{sub}	-1	f_{bio}									$1-f_{bio}$	$k_{dis} X_{sub}$	
2		Hydrolysis of X_f		-1	1									$k_{hyd} \frac{X_f/X_B}{K_x + X_f/X_B} X_B$	
3		Sugars Uptake			-1	$(1-Y_B)f_{ac}$	$(1-Y_B)f_{pro}$	$(1-Y_B)f_{bu}$	$(1-Y_B)f_{H_2}$	$(1-Y_B)f_{others}$	Y_B			$k_m \frac{S_f}{K_s + S_f} X_B$	
4		Decay		f_f								f_s	$1-f_s-f_f$	$b X_B$	
		Stoichiometric parameters: Fraction of fermentable substrate: f_{bio} Biomass yield: Y_B Fraction of methabolized COD for product formation: f_i Fraction of biomass yielding particulate products: f_s Fraction of biomass yielding fermentable particulate products: f_f													Kinetic parameters: Disintegration of substrate: k_{dis} Sucrose hydrolysis: k_{hyd} , K_x Biomass growth on hexoses: k_m , K_s Biomass decay: b
															Particulate organics (gCOD/l) Biomass (gCOD/l) Lactate and alcohols (gCOD/l) Hydrogen gas (gCOD/l) Butyrate (gCOD/l) Propionate (gCOD/l) Acetate (gCOD/l) Fermentable substrate (gCOD/l) Substrate biodeg. COD (gCOD/l) Total substrate COD (gCOD/l)
															Particulate inerts (gCOD/l)

3.1 Implementation on AQUASIM 2.1

The program AQUASIM was designed for the identification and simulation of aquatic systems and have wide range of applications, from laboratory setups to technical plants and natural environments. The program provides a graphical user interface and uses a communication language familiar to environmental scientists. AQUASIM allows the user to specify transformation processes and, in addition to perform simulations, it offers elementary methods for parameter identifiability analysis, for parameter estimation and for uncertainty analysis (Reichert, 1998).

A model, in the program, consists of ordinary and/or partial differential equations and algebraic equations, which enable to describe the behaviour of a given set of state variables. The differential equations for water flow and substance transport are implemented in compartments, environmental and technical ones, which can be chosen and connected by links. All the transformation processes can be defined by a set of process rates describing the temporal variation of a given substance's concentration. Two process types can be set: dynamic and equilibrium processes. AQUASIM offers therefore, to build a model utilizing four subsystems, i.e. variables, processes, compartments and links, which are mutual dependent one on the other. It is obvious that variables constitute the basic subsystem required for the formulation of the model; their proper definition is essential and represent the first step in the scheme formulation. Processes arrive just after; they have to be defined before to be activated in compartments. Finally, links connect the defined compartments, which are design to spatially divide the system under investigation (Reichert, 1998).

The presented model was built considering a unique group of bacteria whose activities have been formulated into 11 dynamic state variables and 4 kinetic bioconversion processes. The system was implemented in AQUASIM 2.1 as a constant volume mixed liquid compartment without considering gas-liquid transfer processes but pretending that the hydrogen produced is directly present in its gaseous form and is, thus, immediately released in the gas phase. In addition, other physicochemical processes like acid-base reactions and pH calculations were not taken into consideration in this first formulation.

3.1.1 Variables

Dynamic state variables have been the first to be defined as they constitute the core of the model and enable to describe the biological system. These variables are calculated at a specific time (t)

by solution of the set of differential equations as subsequently defined by the process rates, the modelled configuration, inputs and initial conditions assigned. In AQUASIM dynamic state variables are divided into dynamic volume state variables and dynamic surface state variables. The ones of interest for this model are the former, which are used to describe concentration of substances transported with the water flow and quantified as mass per unit volume of liquid. The eleven dynamic volume state variables implemented in the model are presented in the following table.

Table 3-3. Dynamic state variables characteristics

Name	Description	Units	MW	$\text{g}_{\text{COD}} \text{mole}^{-1}$
S_ac	acetate	$\text{g}_{\text{COD}} \text{L}^{-1}$	60	64
S_bu	butyrate	$\text{g}_{\text{COD}} \text{L}^{-1}$	88	160
S_pro	propionate	$\text{g}_{\text{COD}} \text{L}^{-1}$	74	112
S_ch	carbohydrates	$\text{g}_{\text{COD}} \text{L}^{-1}$	varies	varies
S_h2	hydrogen	$\text{g}_{\text{COD}} \text{L}^{-1}$	2	16
S_mo	monosaccharides	$\text{g}_{\text{COD}} \text{L}^{-1}$	180	192
S_others	lactate, alcohols	$\text{g}_{\text{COD}} \text{L}^{-1}$	varies	varies
S_s	soluble organics	$\text{g}_{\text{COD}} \text{L}^{-1}$	varies	varies
X_B	biomass	$\text{g}_{\text{COD}} \text{L}^{-1}$	120	170
X_i	particulate inerts	$\text{g}_{\text{COD}} \text{L}^{-1}$	varies	varies
X_s	particulate organics	$\text{g}_{\text{COD}} \text{L}^{-1}$	varies	varies

Afterwards, the program variables, which refer to predefined quantities of the system, were edited.

Besides the time coordinate (t) the volume of the reactor (V) was defined.

All the parameters, kinetics, yields and fractions were implemented as constant variables. Constant variables can be used to describe single measured quantities, with assigned values and standard deviations or can be used as model parameters and let the program to estimate them. Figure 7 shows the dialog box of AQUASIM 2.1 used for defining or editing a constant variable, in the specific case is the first order constant of the hydrolytic step.

Figure 7. Dialog box for editing a constant variable

The measured quantities defined as a function of other variables, such as the temporal profiles of hydrogen and VFAs, are represented by real list variables. To implement real list variables the argument, a list of argument-value data pairs, the standard deviations of the data and the interpolation method must be specified (Figure 8). Once defined, a real list variable that have the time program variable as argument can be used as target for parameters estimation. In this case, the variable to be compared with the real list is evaluated at the positions of the data pairs and the differences between the values of the two variables are summed up according to equation (15) using the standard deviations specified for the real list variable (Reichert, 1998).

Argument	Value	Std. Deviation	Pairs:
0.6528	0.814	0.1644	6
1.0069	0.8721	0.2138	
1.6542	0.9651	0.1788	
2.7222	1.1442	0.1581	
5.7049	1.1754	0.1517	
7.6	1.2172	0.1916	

Figure 8. Dialog box for editing a real list variable

The last typology of variables present in the model are the formula variables, which allow to build functional relations as algebraic expressions using previously defined variables. An example is presented in Figure 9 where the product yield of the acetic acid is defined.

Figure 9. Dialog box for editing a formula variable

3.1.2 Processes

The model includes the biochemical step of acidogenesis (fermentation) as well as the extracellular disintegration and hydrolysis. Two processes, implemented as sugars uptake and biomass decay, describe the fermentation step. The uptake process has a number of parallel reactions, including biomass growth and products formation. While the uptake is based on substrate level Monod-type kinetics, the biomass decay to composite material, was assumed as a first order reaction and is described with an independent expression.

The four processes defined in the model are dynamic; therefore, the substance transformations are described along the time scale of the simulation. In AQUASIM, the process rate is separated as common factor in the process while the stoichiometric coefficients are defined for each substance involved. The contribution of a process to the temporal variation of the concentration of a substance is then given as the product of the common process rate and the specific stoichiometric coefficient (Reichert, 1998). This method of presentation of dynamic biochemical processes is associated to a stoichiometric matrix as the one presented in (Table 3-2).

In Figure 10 is shown the dialog box used for defining or editing a dynamic process, in this case the uptake.

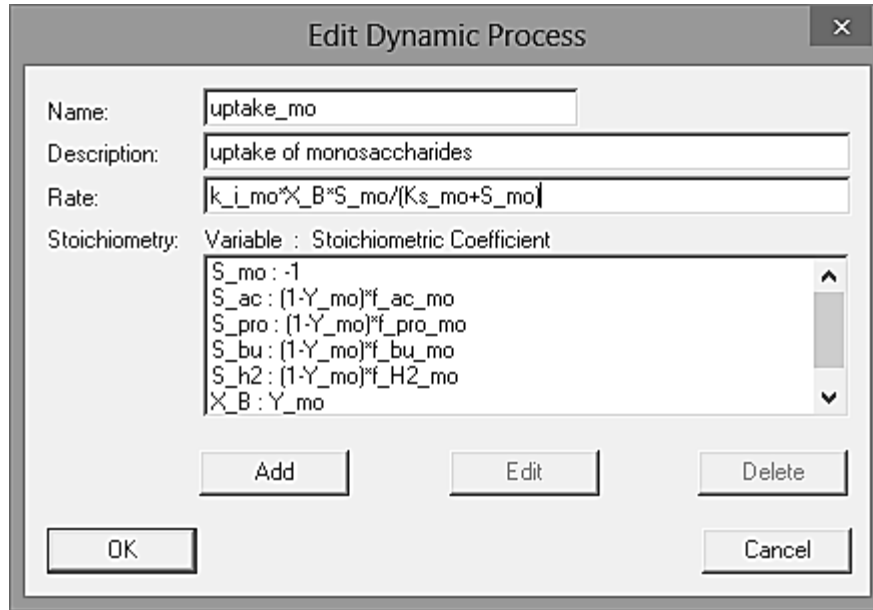


Figure 10. Dialog box for editing a dynamic process

3.1.3 Compartments

The geometrical composition of an AQUASIM system consists of a set of compartments of given types. In the presented model, a mixed reactor compartment was chosen. It describes inflow, outflow and transformation processes in a completely stirred reactor with constant volume.

Thus, the temporal change of the concentration of substances dissolved or suspended in the water, considering just the state variables included in the uptake process, is given as

$$\frac{d}{dt} \begin{bmatrix} Glu \\ Ace \\ Pro \\ Bu \\ Others \\ H_2 \\ X_B \end{bmatrix} = Kr - D \begin{bmatrix} Glu - Glu_{in} \\ Ace \\ Pro \\ Bu \\ Others \\ H_2 \\ X_B \end{bmatrix} \quad (13)$$

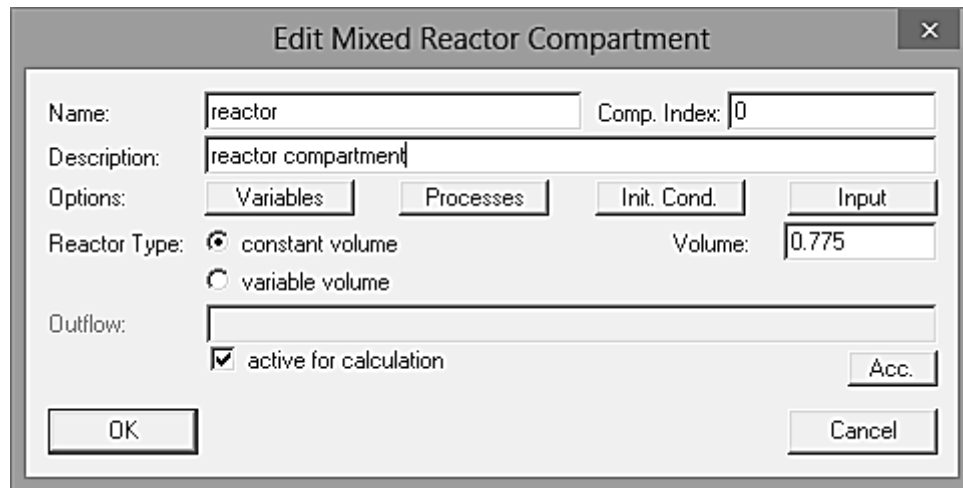
The equation (13) represents the overall mass balance when glucose is considered as representative monosaccharide. *Glu*, *Ace*, *Pro*, *Bu*, *H₂* and *X_B* represent respectively the concentration in g_{COD} L⁻¹ of glucose, acetate, propionate, butyrate hydrogen and biomass in the liquid phase while other bio-products such as lactate and alcohols are included as *Others*. The vector *r* represents the kinetics of the involved biological reactions (in g_{COD}L⁻¹d⁻¹), *K* represents the matrix of pseudo-stoichiometric coefficients and *D* is the dilution rate (d⁻¹).

Once selected the type of compartment and specified the volume, state variables and processes of interest must be activated. Subsequently, the initial condition for each active state variable can be specified.

The initial concentration of active biomass, i.e. acidogenic bacteria, was estimated during the calibration step being not possible to forecast the amount of bacteria able to survive and re-activate after the heat pretreatment step. Thus, a constant value variable was set as initial biomass concentration in the reactor compartment.

For the estimation of the COD equivalents of microbial biomass, the oxidation equation of the empirical formula $C_5H_7O_2N$ was used, obtaining a conversion factor of $1.42 \text{ g}_{COD}/\text{g}_{VSS}$ which is well in the range of experimentally determined values (Contreras et al., 2002).

As can be seen in Figure 11, inputs to the mix reactor compartment can also be defined from the dialog box. Once selected the water inflow (which can be either constant or a real list variable) one unique loading, expressed as mass per unit of time, can be specified for each variable.



The dialog box is titled "Edit Mixed Reactor Compartment" and contains the following fields and controls:

- Name: reactor
- Comp. Index: 0
- Description: reactor compartment
- Options: Variables, Processes, Init. Cond., Input
- Reactor Type: constant volume, variable volume
- Volume: 0.775
- Outflow: (empty field)
- active for calculation
- Buttons: OK, Cancel, Acc.

Figure 11. Dialog box for editing a mixed reactor compartment

The model variables and equations implemented are solved by AQUASIM using the algorithm DASSL which is based on the implicit variable-step, variable-order Gear integration technique (Reichert, 1998). The numerical integration was performed with a time step of 0.1 days.

For modelling both the batch and the CSTR experimental setups, just one compartment was defined, which is a mixed reactor compartment type and where all the eleven variables and four processes were active. In the continuous mode, the reactor has a single input and output stream with constant liquid volume. The inflow and the substrate load are dynamic, set as a real list variable, since they changed during the experimental trial. In the batch mode, the inflow is set to zero, thus the dilution rate in equation (13) is null and the model simulates the variation over the time of the state variables due to biochemical reactions only.

Initial concentrations were defined, different from zero, for the initial active biomass and for the substrate, while the remaining dynamic state variables initial concentration was set null.

3.1.4 Sensitivity analysis and parameter estimation

To study the uncertainty in the output of the model and the identifiability of the parameters a sensitivity analysis has to be done. The sensitivity function selected on AQUASIM is the absolute-relative function (14), which measures the absolute change in y for a 100% change in p . Where y is the variable and p the parameter.

$$\delta_{y,p}^{a,r} = p \frac{\delta y}{\delta p} \quad (14)$$

The linear approximation to the change in y for 100% change in p can easily be constructed with the aid of the tangent to the function $y(p)$ in p . The larger the values of the sensitivity functions and the more pronounced are the differences in shape, the more accurately are the parameters identifiable (Reichert, 1998). Once individuated the parameters on which the variables of interest are more sensitive and the correlations between different parameters, the calibration step can be performed.

Values for kinetic parameters and constants that were suggested by Batstone et al. (2002) in their original model report, have been used as a base line for the parameters estimation.

AQUASIM estimates the model parameters by minimizing the sum of the squares of the weighted deviations between measurements and calculated model results (Reichert, 1998).

$$\chi^2(p) = \sum_{i=1}^n \left(\frac{y_{meas,i} - y_i(p)}{\sigma_{meas,i}} \right)^2 \quad (15)$$

In equation (15), $y_{meas,i}$ is the i -th measurement, $\sigma_{meas,i}$ is its standard deviation, $y_i(p)$ is the calculated value of the model variable corresponding to the i -th measurement and evaluated at the time and location of this measurement, $p = (p_1, \dots, p_m)$ are the model parameters and n is the number of data points. The standard deviations have been defined individually for each data point of the real list variables in the batch tests while they were defined globally in the continuous test. The sum is then minimized numerically using the simplex algorithm, implemented on AQUASIM and selected in the dialog box for parameter estimation Figure 12.

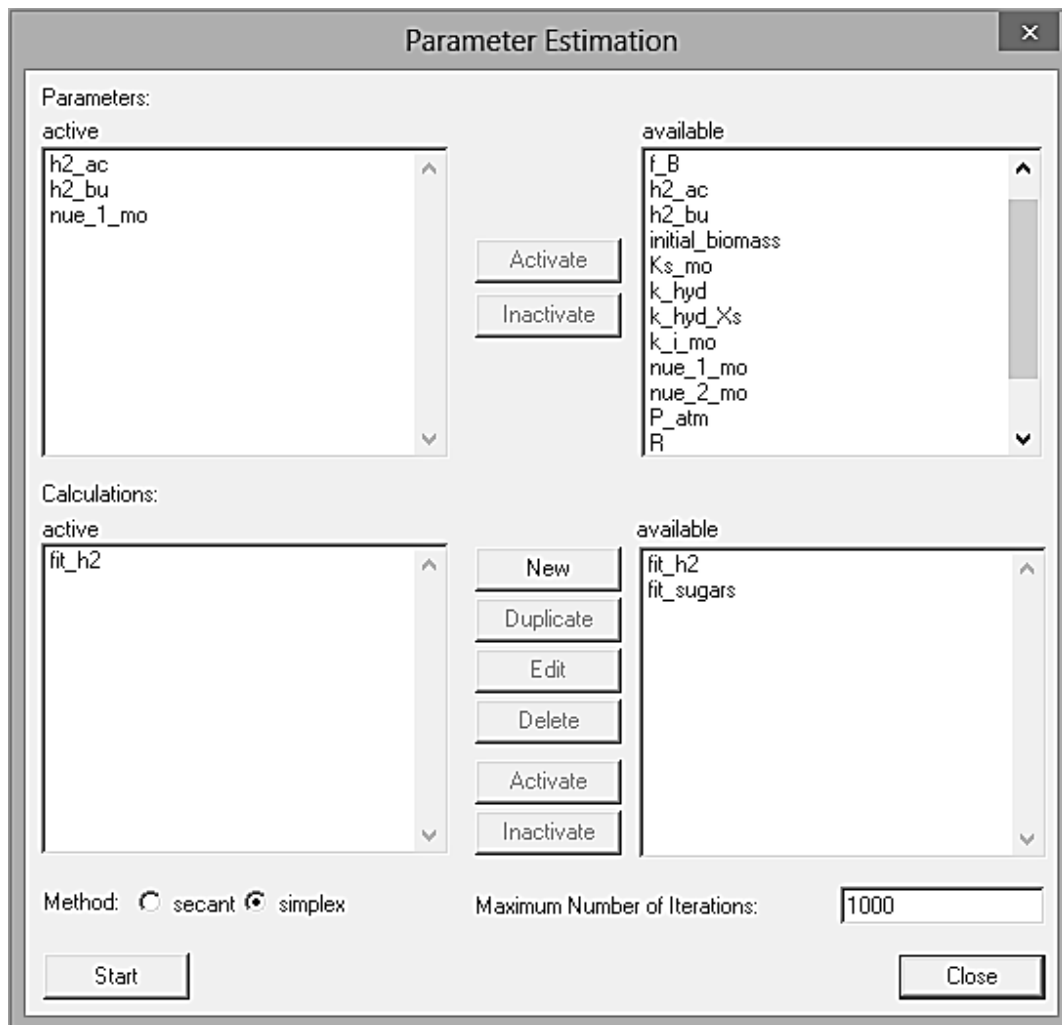


Figure 12 Dialog box for editing a parameter estimation.

The values of the estimated parameters were then discussed and compared to available literature data derived from reviews of previous fermentative hydrogen production model works.

4 RESULTS AND DISCUSSION

In the tests performed with heat-treated anaerobic sludge, methane was not detected in any of the reactors, in both batch and continuous configurations, confirming that the pre-treatment was adequate to suppress methanogens and validating the assumption of the model. Moreover, in all the blanks, where just the seed sludge was present, no hydrogen production was observed.

In presenting the results of the model calibration the batch tests are listed from the simplest substrate utilized (glucose) to the most complex (wheat bran). Then the CSTR implementation is discussed.

4.1 Sensitivity analysis

Since the model parameters were established by a curve-fitting process, a sensitivity analysis was performed on each of the parameters to discern their impact on the predicted production of hydrogen and VFAs. The absolute-relative sensitivity function (14), implemented on AQUASIM (Reichert, 1998), was utilised since it does not depend on the unit of the parameters. This enable to make a quantitative comparison of the effects of different parameters on a common variable. The sensitivity functions of the calculated hydrogen production and VFAs generation with respect to the three kinetic parameters K_s , k_m , k_d and the *initial active biomass*, are presented in Figure 13.

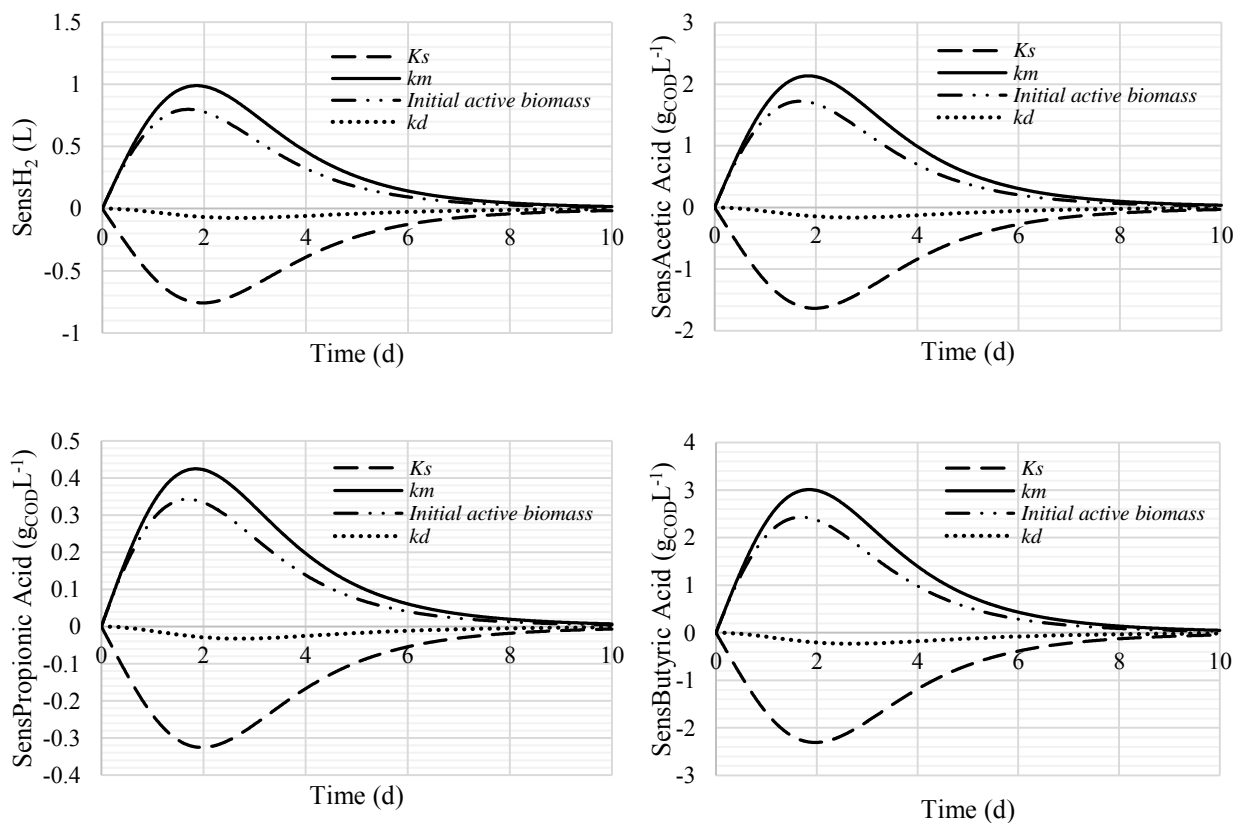


Figure 13. Sensitivity functions of hydrogen, acetic, propionic and butyric acid generation with respect to the kinetic parameters K_s , k_m and k_d and to the initial active biomass.

The analysis were conducted on the glucose batch test but the considerations can be extended to all the simulations, since the structure of the model is unchanged.

The sensitivity functions of the four variables calculated (hydrogen volume, acetic acid, propionic acid and butyric acid concentration) are identical; therefore, the parameters under investigation effect in the same way the hydrogen and the VFAs production.

It is evident the much smaller sensitivity of the simulated volume and concentrations to the parameter k_d in comparison to the other parameters. It leads to a larger uncertainty of the estimation of k_d , as will be discussed later starting from the value of the standard error in Table 4-1.

The sensitivity functions of the variables to the other three parameters have a similar shape. The calculated volume of hydrogen and the VFAs concentrations increase with increasing values of initial active biomass and k_m , but they decrease with increasing values of K_s . This leads to a correlation between the estimates of these parameters; changes in calculated concentrations caused by a variation in *initial biomass* or k_m can approximately be compensated by an appropriate change in K_s . The sensitivity functions of the calculated hydrogen production and VFAs generation with respect to five metabolic parameters have also been calculated (Figure 14, Figure 15 and Figure 17). Again, the absolute-relative sensitivity function has been used.

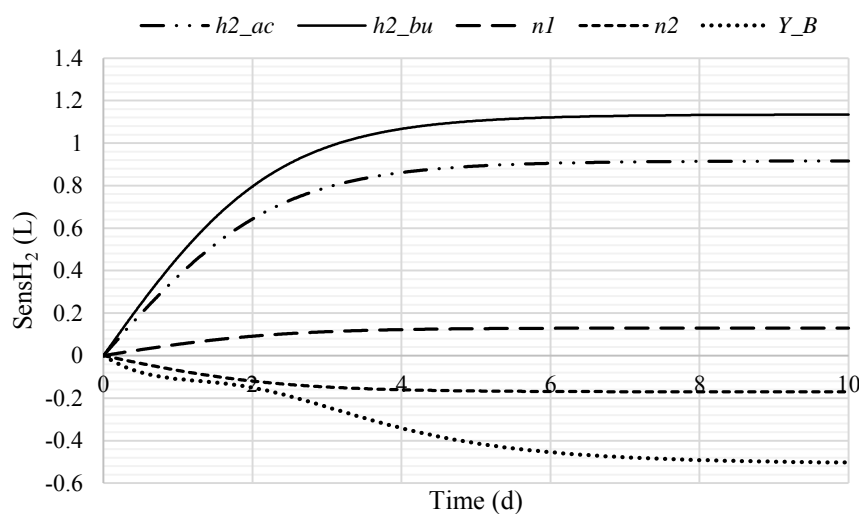


Figure 14. Sensitivity functions of hydrogen generation with respect to the metabolic parameters $h_{2,ac}$, $h_{2,bu}$, n_1 , n_2 and Y_B .

The shape of the function relative to the biomass yield (Y_B) is the same in this and all the following figures (from 14 to 17) meaning that hydrogen and VFAs are affected similarly by a change of this variable. Incrementing the value of Y_B the production of metabolites decreases proportionally.

The sensitivity functions of the other parameters in Figure 14 have a similar shape. Increasing the value of n_2 the calculated volume of hydrogen decreases. This parameter represents in fact the reaction leading to the formation of acetate and propionate without hydrogen generation. The

estimation of this parameter is correlated to the estimation of n_1 , $h_{2,ac}$ and $h_{2,bu}$. Changes in produced volume of hydrogen caused by a variation of n_2 , can be compensated by an appropriate change of either n_1 , $h_{2,ac}$ or $h_{2,bu}$. The larger values of the sensitivity functions on the parameters representing the hydrogen yields ($h_{2,ac}$ and $h_{2,bu}$) indicate the higher influence of these parameters on the variable under consideration. Moreover, leads to a higher accuracy in the estimation of the parameters themselves.

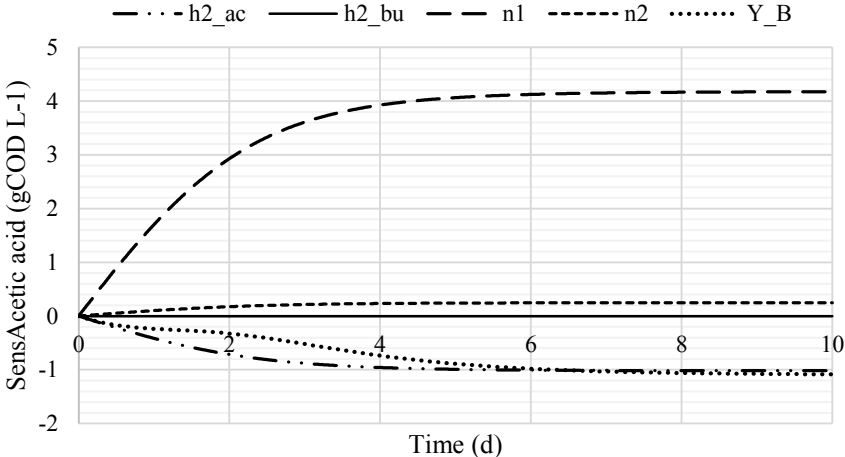


Figure 15. Sensitivity functions of acetic acid generation with respect to the metabolic parameters $h_{2,ac}$, $h_{2,bu}$, $n_{1,mo}$, $n_{2,mo}$ and Y_B .

Figure 15 shows the sensitivity functions of acetic acid generation to five metabolic parameters. The calculated concentration of acetic acid is not sensitive at all to $h_{2,bu}$. This parameter represents the hydrogen yield on the butyric acid generation pathway, as expected is not affecting acetic acid production. On the other hand, the increasing values of $h_{2,ac}$, the yield of hydrogen on the acetic acid generation, lead to a decrease of acid concentration. This can be compensated by an appropriate change of n_1 and to a minor extent of n_2 . Both the latter parameters represent catabolic reactions with acetic acid generation.

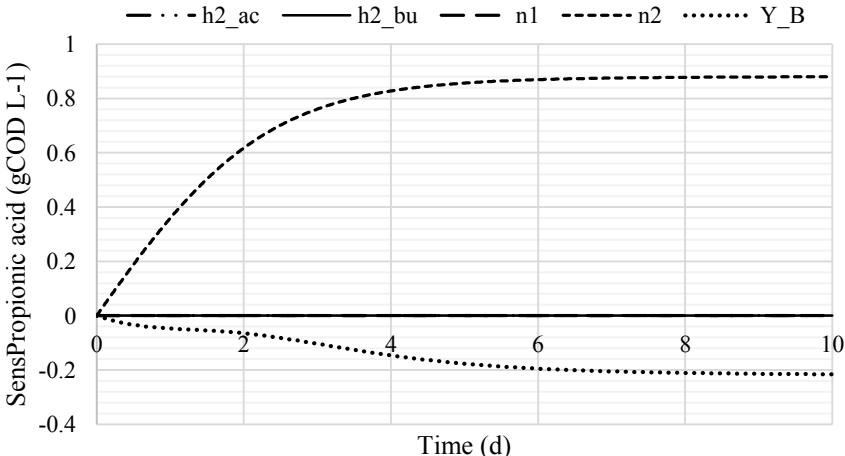


Figure 16. Sensitivity functions of propionic acid generation with respect to the parameters $h_{2,ac}$, $h_{2,bu}$, $n_{1,mo}$, $n_{2,mo}$ and Y_B .

Figure 16 shows the sensitivity functions of propionic acid generation with respect to the metabolic parameters. A part from the function of the parameter Y_B , which effects equally the generation of all metabolites, the concentration of propionic acid is only sensible to the parameter n_2 that represent the only catabolic reaction leading to propionic acid generation.

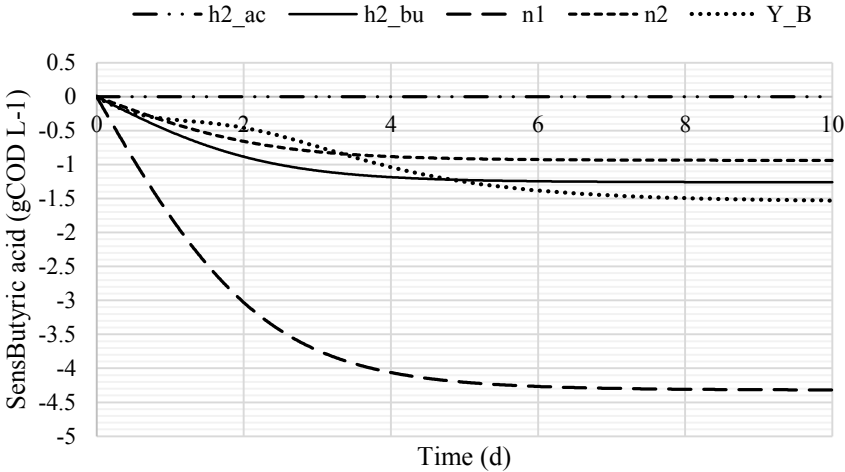


Figure 17. Sensitivity functions of butyric acid generation with respect to the metabolic parameters $h_{2,ac}$, $h_{2,bu}$, $n_{1,mo}$, $n_{2,mo}$ and Y_B .

The butyric acid concentration have sensitivity functions, with respect to the metabolic parameters under consideration, with negative values (Figure 17). The calculated concentration decrease with increasing values of $h_{2,bu}$, n_1 and n_2 while is not sensitive to the parameter $h_{2,ac}$. The parameters are not correlated to each other and the variable considered is mostly sensitive to the parameter n_1 .

From the sensitivity analysis performed, emerges that hydrogen volume and VFAs concentration, which are the variable subsequently used for the calibration, are effected by the kinetic parameters and the initial biomass concentration in the same way; therefore, the calibration of these parameters is reflected on all the state variables considered. On the other hand, the variables presented different sensitivity to the metabolic parameters. The propionic acid concentration, for example, depends mostly on the value of the parameter n_2 while the acetic and the butyric acid concentrations are more sensitive n_1 .

The parameters presenting a correlation are subsequently not calibrated together.

4.2 Model calibration

4.2.1 Model calibration on glucose BHP batch test

The experimental data on hydrogen production and VFAs generation from glucose in batch test were retrieved from literature (Giordano et al., 2011). These data were used for the model parameter estimation. In Table 4-1 the parameters for the glucose batch test are shown. The starting values are those recommended in the ADM1 framework. The best-fit parameters, estimated through curve-fitting process are listed with the standard errors. Furthermore, kinetic parameters from literature have been reported for comparison.

Table 4-1 Model parameters for batch test with glucose

Source	ADM1	Best-fit	Literature
Substrate	Monosaccharides	Glucose	Glucose
Initial substrate (gCODL ⁻¹)	-	19.62	-
Seed sludge(gCODL ⁻¹)	-	56.8	-
Initial active biomass (gCODL ⁻¹)	-	5.56 ± 0.61	-
K _s (gCODL ⁻¹)	0.5	36.25 ± 5.97	11.89-17.23 ^{[1]-[2]}
f _{bio}	-	1	-
k _m (d ⁻¹)	30	4.74 ± 0.39	-
μ _{max} (gCOD _s gCODX ⁻¹ d ⁻¹)	3	0.9 ± 0.28	0.03-9.6 ^{[2]-[1]}
k _d (d ⁻¹)	0.02	0.13 ± 0.09	1.02 ^[3]
nue _{1_mo}	0.495	0.38 ± 0.03	-
nue _{2_mo}	0.345	0.08 ± 0.02	-
h _{2_ac}	0.33	0.20 ± 0.06	-
h _{2_bu}	0.17	0.17 ± 0.04	-
r _{acid}	-	0.84 ± 0.04	-
Y _B (gCODX gCOD _s ⁻¹)	0.1	0.19 ± 0.04	0.184-0.195 ^{[4]-[3]}

[1] Chittibabu et al., 2006; [2] Sharma and Li, 2009; [3] Ntaikou et al., 2009; [4] Nath, 2008.

The estimated parameters have been use to perform a simulation of the system. The hydrogen produced and the VFAs generated are visible in the following charts.

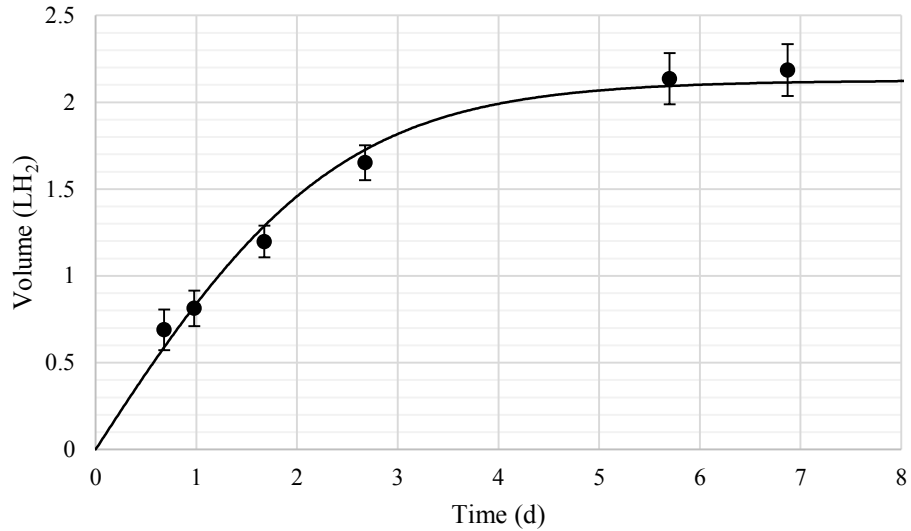


Figure 18 Cumulative hydrogen production. Experimental values (●) with standard deviation.

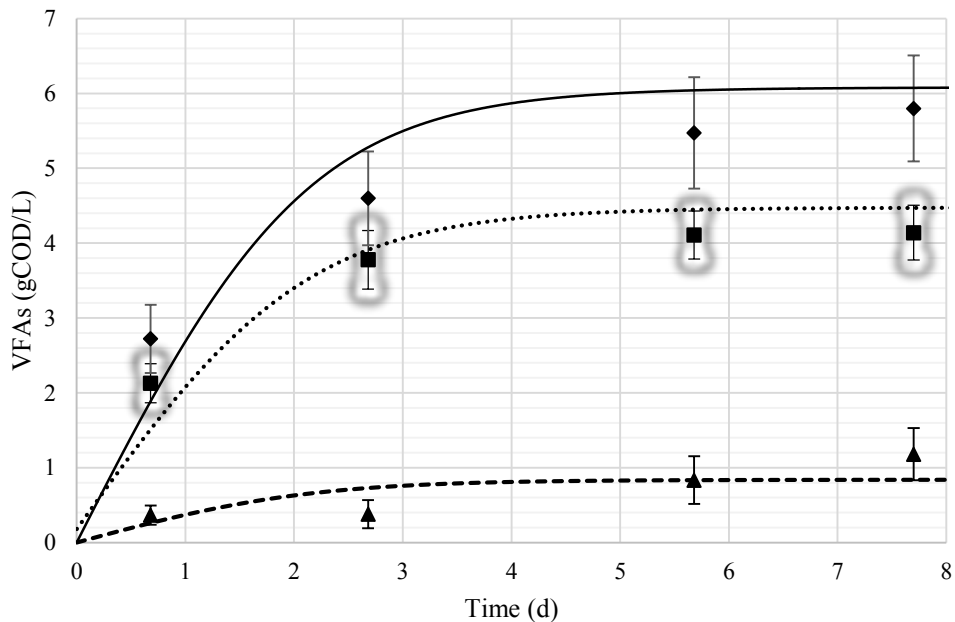


Figure 19 Measured vs predicted VFAs profiles. Symbols represent measured values with the error bars showing the standard deviation. Symbols: butyric (◆) acetic (■) and propionic (▲) acid.

Figure 18 reports the simulated cumulative hydrogen production and the experimental values with error bars displaying the standard deviations. Figure 19 shows the VFAs concentration as COD. The values of COD per unit mass of acetate, propionate and butyrate, used to plot the measured concentrations, are $1.067 \text{gCOD g}_{\text{acetate}}^{-1}$, $1.514 \text{gCOD g}_{\text{propionate}}^{-1}$ and $1.818 \text{gCOD g}_{\text{butyrate}}^{-1}$.

As expected, the estimated parameters differ from those proposed by Batstone et al. (2002). The values suggested for the application of the ADM1 refer to monosaccharides degradation by

acidogens in a syntrophic network that leads to methane production. In dark fermentation the conditions are quite different and, thus, the parameters involved assume different values.

The estimated kinetic parameters for the growth on glucose are closed to those found in literature for models using classical Monod kinetics (Chittibabu et al., 2006; Sharma and Li, 2009) and Monod kinetics with inhibition corrections for pH and substrate (Nath, 2008; Ntaikou et al., 2009). As can be seen from Table 4-1 the maximum specific growth rate found in literature varies between two orders of magnitude. This is not surprising being that the microorganisms involved in those studies are different. Moreover, the maximum specific growth rate is temperature and pH dependent. Although temperature is usually kept constant during the experiments, pH can be either controlled or not. This might result in the differences of μ_{\max} value.

The comparison of kinetic parameters coming from literature is difficult because of the heterogeneity of the fermentative microorganisms, the experimental conditions and the modelling approaches. The introduction of inhibitory factors in the Monod kinetic, for instance, could bring to an overestimation of the maximum specific growth rate compared to the use of a classical Monod (calibrating on the same data).

The initial active biomass is around 10% of the volatile solids present in the seed sludge. The model has estimated this value during the calibration step since it is not possible to distinguish the alive biomass from the dead one after the pretreatment step.

The half saturation constant (K_s) estimated is higher than the initial available substrate, meaning that the actual growth rate during fermentation is well below the 50% of the maximum. This observation spreads for almost all the modelled substrates. The maximum specific growth rate (μ_{\max}), on the other hand, is in the middle of the literature range. In Table 4-1 it is calculated multiplying the biomass yield coefficient to the maximum uptake rate (k_m).

The value estimated of the decay constant (k_d) has a standard error of the same order of magnitude. This parameter has a high variability when modelling batch test for BHP determination because the rate of change of the biomass is not sensitive to the decay process during the exponential growth that is when almost the entire substrate is consumed and metabolites produced.

The yield coefficient (Y_B) falls perfectly in the middle of the retrieved literature data. Probably, in a fermentative anaerobic environment the amount of biomass growing per mass of substrate has a narrow range of variation.

The values of metabolic coefficients ($n_{1,mo}$ and $n_{2,mo}$) show that the reactions which produce butyric and acetic acids prevail on that producing propionic acid. The hydrogen yields ($h_{2,ac}$ and $h_{2,bu}$) on the former reactions are equivalent to 2.42 and 2 moles of hydrogen per mole of glucose for acetic and butyric acid, respectively. The glucose fraction that is not utilised in bacterial

anabolism and is acidified, is equal to 0.84; therefore, 16 % of the sugar available for the catabolism is converted into other metabolites (solvents) than VFAs.

The model is based on a COD mass balance thus, can be interesting to discuss the fate of the substrate (Figure 20).

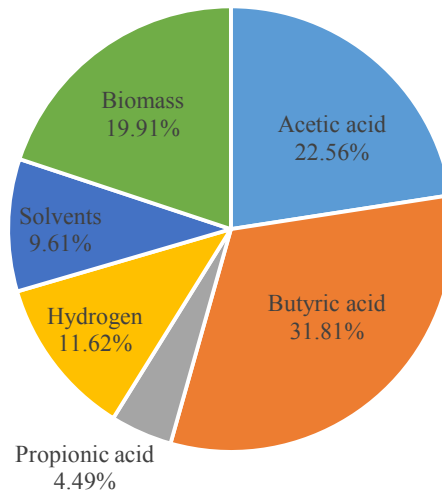


Figure 20 Pie chart showing the input COD fate

The initial COD converted to hydrogen is just the 10% while around 70% is turned into VFAs and solvents and 20% is used by the biomass to grow. The yield of hydrogen on the total glucose is $1.4 \text{ mol}_{\text{hydrogen}} \text{ mol}_{\text{glucose}}^{-1}$, which is comparable with literature results from other batch tests utilising glucose as substrate (Wang and Wan, 2009; Wong et al., 2014).

4.2.2 Model calibration on sucrose BHP batch test

Batch tests utilizing sucrose as substrate at three different F/M ratios were conducted to assess how the model parameters vary to fit the hydrogen production. The starting values of the parameters were those obtained from the glucose calibration. Given the different seed sludge utilized, kinetic values were expected to change. Table 4-2 reports the calibrated parameters with standard errors for the three BHP tests and kinetic parameters retrieved from the literature.

Table 4-2. Model parameters for batch test with sucrose

Source	Best-fit	Best-fit	Best-fit	Literature
Substrate	Sucrose	Sucrose	Sucrose	Sucrose
Initial substrate (g _{COD} L ⁻¹)	9.32	4.66	2.33	-
Seed sludge(g _{COD} L ⁻¹)	5.91	5.91	5.91	-
F/M ratio	2	1	0.5	-
Initial active biomass (g _{COD} L ⁻¹)	2.34 ± 0.07	2.8 ± 0.09	2.67 ± 0.24	-
K _s (g _{COD} L ⁻¹)	13.2 ± 0.72	9.27 ± 0.18	9.27 ± 0.77	1.62 ^[1] -13.5 ^[2]
f _{bio}	1	1	1	-
k _{hyd} (d ⁻¹)	150 ± 20	150 ± 21	220 ± 156	
k _m (d ⁻¹)	9.79 ± 0.25	10.86 ± 0.18	10.86 ± 0.63	
μ _{max} (g _{COD} s g _{CODX} ⁻¹ d ⁻¹)	0.979 ± 0.16	2.17 ± 0.07	2.17 ± 0.1	3.12 ^[3] -5.3 ^[2]
k _d (d ⁻¹)	0.06 ± 0.05	0.05 ± 0.04	0.15 ± 0.14	-
nue _{1_mo}	0.4 ± 0.02	0.45 ± 0.004	0.45 ± 0.012	-
nue _{2_mo}	0.16 ± 0.01	0.16 ± 0.004	0.16 ± 0.013	-
h _{2_ac}	0.28 ± 0.004	0.29 ± 0.001	0.32 ± 0.004	-
h _{2_bu}	0.16 ± 0.006	0.15 ± 0.003	0.13 ± 0.006	-
r _{acid}	0.75 ± 0.007	0.7 ± 0.002	0.42 ± 0.003	-
Y _B (g _{CODX} g _{CODS} ⁻¹)	0.1 ± 0.013	0.2 ± 0.003	0.2 ± 0.006	0.13 ^[4]

[1] C-C. et al., 2001; [2] Chen et al., 2006; [3] Mu et al., 2006; [4] van Niel et al., 2003

The estimated parameters have been use to perform a simulation of the system with the three different initial substrate concentration.

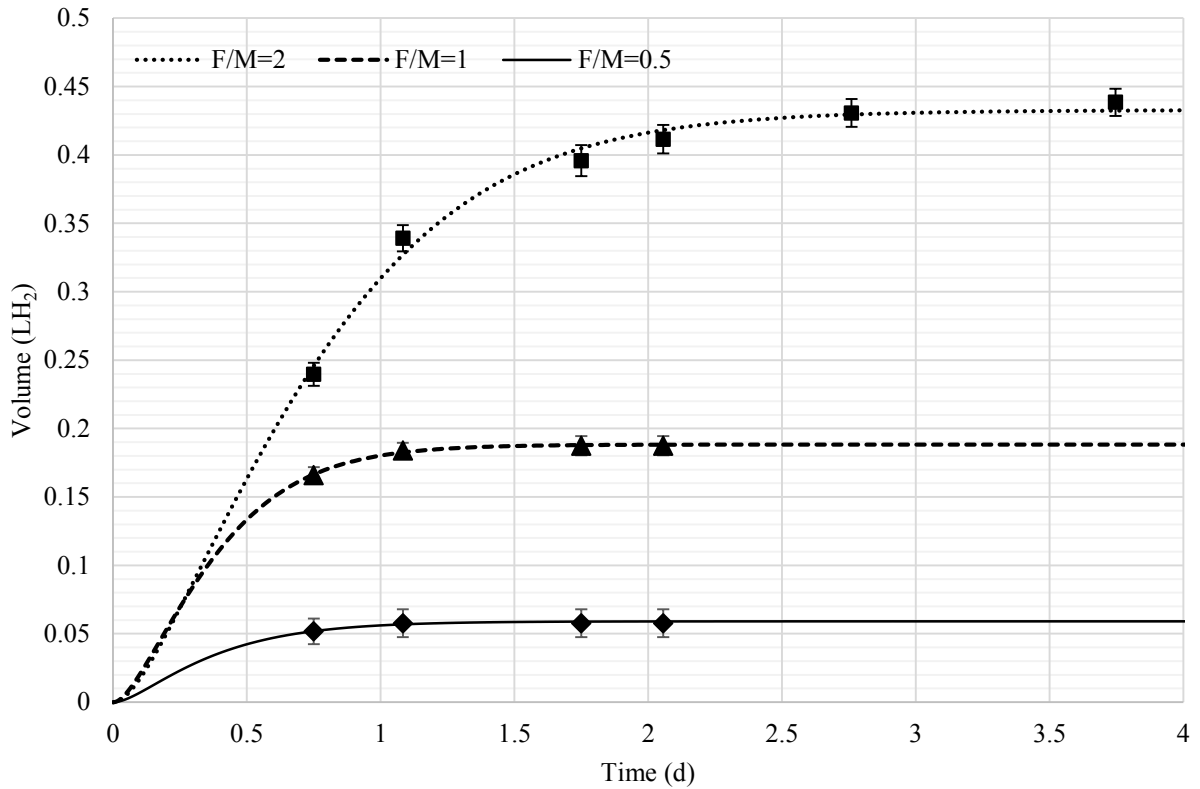


Figure 21. Measured vs predicted hydrogen generation profiles. Symbols represent measured values with the error bars showing the standard deviation. Symbols: F/M=2 (■) F/M=1 (▲) and F/M=0.5 (◆).

Figure 21 shows the three curves of cumulative hydrogen production from the BHP tests. The amount of hydrogen produced is not linearly correlated to the initial substrate concentration. In fact, the H₂ generation is almost tripled when the sucrose concentration is doubled from 2.33 to 4.66 g_{COD} L⁻¹. The increment of the hydrogen yield is less marked when doubling again the concentration of sucrose to 9.32 g_{COD} L⁻¹. Table 4-3 reports the yields of hydrogen production on sucrose degradation calculated from the experimental results and obtained by the model simulation.

Table 4-3 Yields of hydrogen generation on sucrose

F/M ratio	Yield calculated from experimental data			Yield estimated by the model
	(mL _{H2} g _{su} ⁻¹)	(mol _{H2} mol _{su} ⁻¹)	(g _{CODH2} g _{CODsu} ⁻¹)	(g _{CODH2} g _{CODsu} ⁻¹)
2	210.83 ± 4.77	2.85 ± 0.06	0.12 ± 0.003	0.12 ± 0.009
1	180.15 ± 6.78	2.44 ± 0.09	0.10 ± 0.004	0.11 ± 0.006
0.5	110.83 ± 19.60	1.5 ± 0.26	0.06 ± 0.011	0.07 ± 0.004

The model is able to give a solid estimation of the substrate COD fraction ending into hydrogen. Moreover, the yields obtained are similar to results found in literature (Davila-Vazquez et al., 2008).

As for the calibration with data from glucose fermentation, the model has estimated the initial active biomass. Since the three batch tests with sucrose were seeded with the same amount of pretreated anaerobic sludge, the values of the concentration of initial biomass estimated by the model result similar (Table 4-3).

The half saturation constant (K_s) is comparable to the values found in literature. It is higher than the initial concentration of substrate in all the three calibrations. The maximum uptake rate (μ_{max}) is thus, never reached during the simulations.

Sucrose is a disaccharide easily hydrolysable. The hydrolytic constant (k_{hyd}) is one order of magnitude higher than the uptake rate (k_m). The relevant standard deviation of k_{hyd} is due to this difference in kinetics. The model estimate the hydrolytic parameter with a consistent error especially in the lowest F/M ratio. Here, the concentration of sucrose is low and even if it is hydrolysed at a rate closer to the maximum uptake (the lowest values of k_{hyd} is 64 d⁻¹) the hydrolytic step is still not the bottleneck of the bioconversion. Therefore, even a consistent variation of the hydrolysis rate do not affect the microbial metabolism.

The maximum specific growth rate (μ_{max}) is similar to the values from literature and it is slightly lower in the simulation with the higher sucrose concentration. This can be due to the lower biomass yield compared to the lower F/M ratios. It seems that at higher substrate concentration the biomass is utilizing less COD for the anabolism, yielding more metabolites. The values of the biomass yields estimated are similar to the literature ones. Moreover, looking at the parameter r_{acid} , at higher concentration of substrate the fraction of sucrose turned into VFAs is the 75%. This fraction is similar for the median substrate concentration but drops down at the lowest F/M ratio. On the other side, the hydrogen yields ($h_{2,ac}$ and $h_{2,bu}$) on the acidogenic reactions performed at low substrate concentration are higher than the ones occurring at higher sucrose concentration. In the batch test with F/M equal to 0.5, $h_{2,ac}$ and $h_{2,bu}$ are equivalent to 3.88 and 1.53 moles of hydrogen per mole of monosaccharide through acetic and butyric acid generation, respectively. Instead, with F/M ratios of one and two, the generation of acetate is yielding 3.4 moles of H₂ per mole of hexose and through the butyrate path, 1.76 moles of H₂ per mole of hexose are produced.

The decay rate constant estimated from the model is almost the same for the two tests with higher substrate concentrations and is higher in the other one. However, the standard error is similar to the parameters' values themselves, showing once again how the decay rate is not significant in simulating batch tests with readily biodegradable substrates.

4.2.3 Model calibration on mashed potatoes and potatoes peels BHP batch tests

Batch tests to determine the BHP of two typical wastes of the potato-processing industry were conducted by Giordano et al. (2011). In particular, the two sources were the steam-peeling potato processing and the industrial production of mashed potatoes.

Both the food wastes have a high carbohydrates content. Their dry weight is composed mainly by starch, which account for the 70% in mashed potatoes and 40% in potato peels (Phyllis2 - ECN Phyllis classification). A high degree of degradability is thus expected from the two substrates.

The model parameters were calibrated to fit the hydrogen production and the VFAs generation.

The starting values for the parameters estimation were those obtained from the glucose calibration.

Table 4-4 shows the calibrated parameters with standard errors for the two BHP tests.

Table 4-4 Model parameters for batch test with mashed potatoes and potato peels industrial food wastes.

Source	Best-fit	Best-fit
Substrate	Mashed potatoes	Potato peels
Initial substrate ($\text{g}_{\text{COD}}\text{L}^{-1}$)	10.5	11.4
Seed sludge($\text{g}_{\text{COD}}\text{L}^{-1}$)	56.80	56.80
Initial active biomass ($\text{g}_{\text{COD}}\text{L}^{-1}$)	5.96 ± 0.44	5.87 ± 0.16
K_s ($\text{g}_{\text{COD}}\text{L}^{-1}$)	20.27 ± 1.82	5.55 ± 0.24
f_{bio}	0.89 ± 0.03	0.73 ± 0.01
k_{hyd} (d^{-1})	98.87 ± 87.44	97.21 ± 14.65
k_m (d^{-1})	4.48 ± 0.3	4.15 ± 0.01
μ_{max} ($\text{g}_{\text{CODs}} \text{g}_{\text{CODX}}^{-1} \text{d}^{-1}$)	0.54 ± 0.2	0.5 ± 0.04
k_d (d^{-1})	0.02 ± 0.128	0.02 ± 0.07
nue_1_mo	0.37 ± 0.02	0.41 ± 0.005
nue_2_mo	0.08 ± 0.014	0.11 ± 0.004
h_2_{ac}	0.19 ± 0.017	0.15 ± 0.007
h_2_{bu}	0.16 ± 0.012	0.15 ± 0.006
r_{acid}	0.96 ± 0.03	0.88 ± 0.008
Y_B ($\text{g}_{\text{CODX}} \text{g}_{\text{CODs}}^{-1}$)	0.12 ± 0.038	0.12 ± 0.009

The estimated parameters have been use to perform a simulation of the two batch systems starting from similar initial COD concentration, $10.5 \text{ g}_{\text{COD}}\text{L}^{-1}$ of mashed potatoes and $11.4 \text{ g}_{\text{COD}} \text{L}^{-1}$ of

potato peels. The following figures show the simulations of cumulative hydrogen production, VFAs concentration build up and substrate utilization.

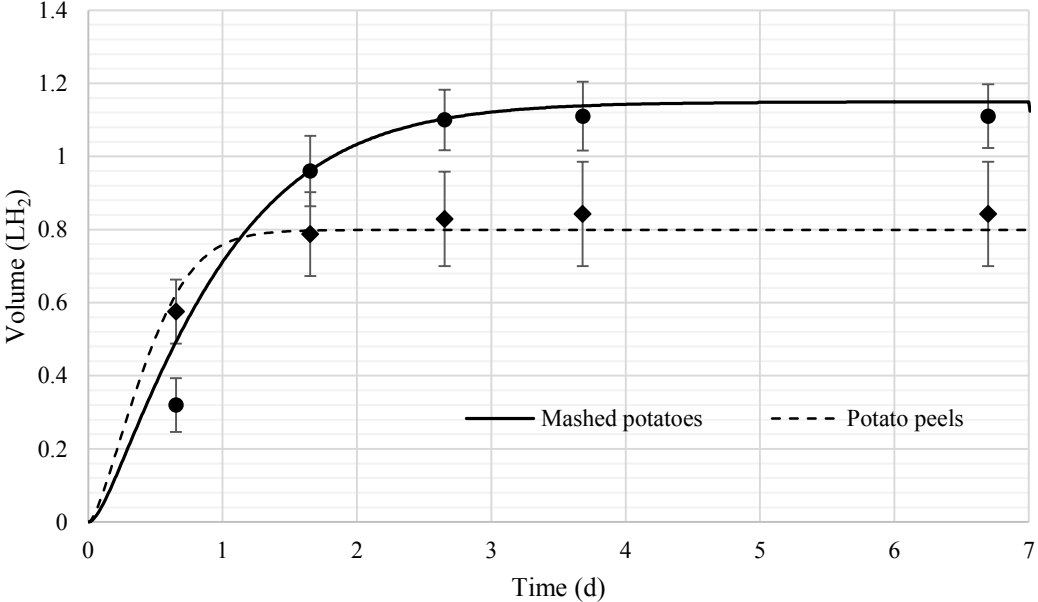


Figure 22. Measured vs predicted hydrogen generation profiles. Symbols represent measured values with the error bars showing the standard deviation. Symbols: Mashed potatoes (●) and potato peels (◆).

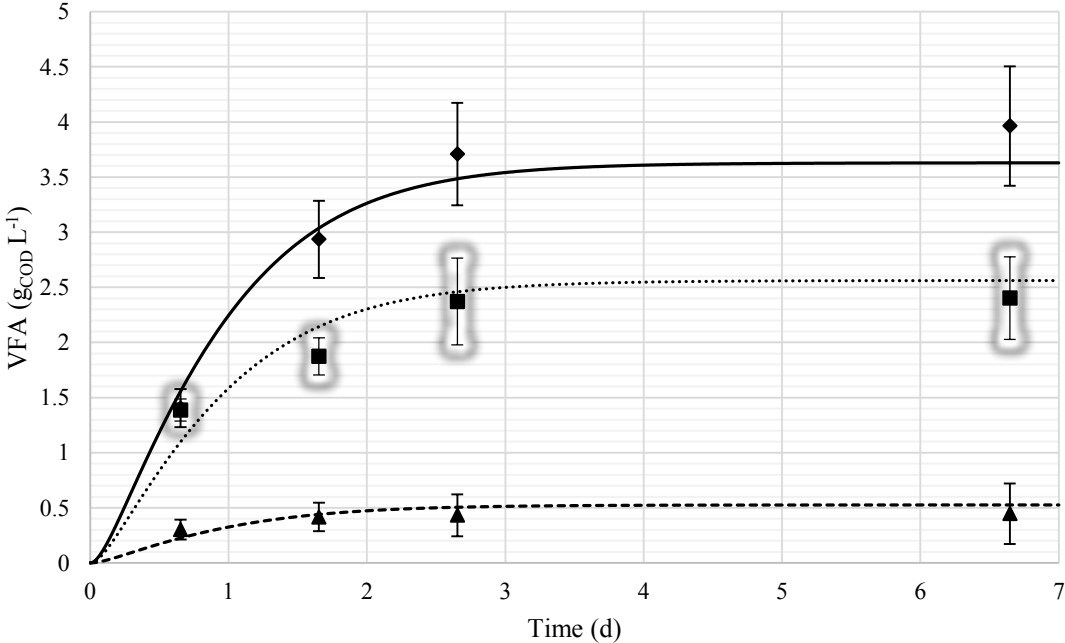


Figure 23. Mashed potatoes: measured vs predicted VFAs profiles. Symbols represent measured values with the error bars showing the standard deviation. Symbols: butyric (◆) acetic (■) and propionic (▲) acid.

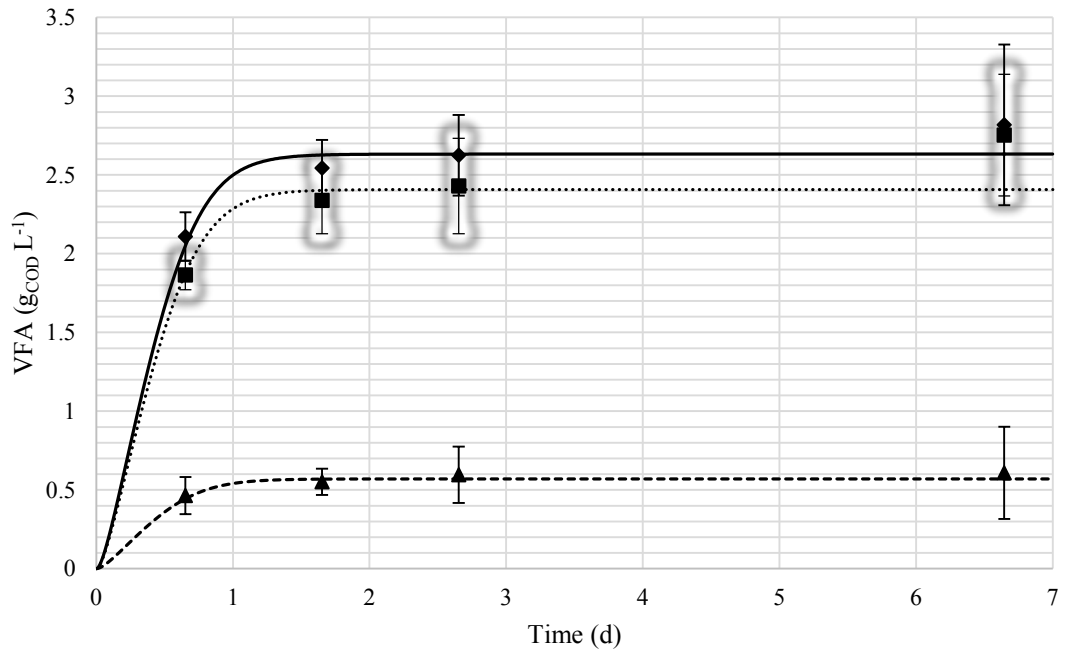


Figure 24. Potato peels: measured vs predicted VFAs profiles. Symbols represent measured values with the error bars showing the standard deviation. Symbols: butyric (◆) acetic (■) and propionic (▲) acid.

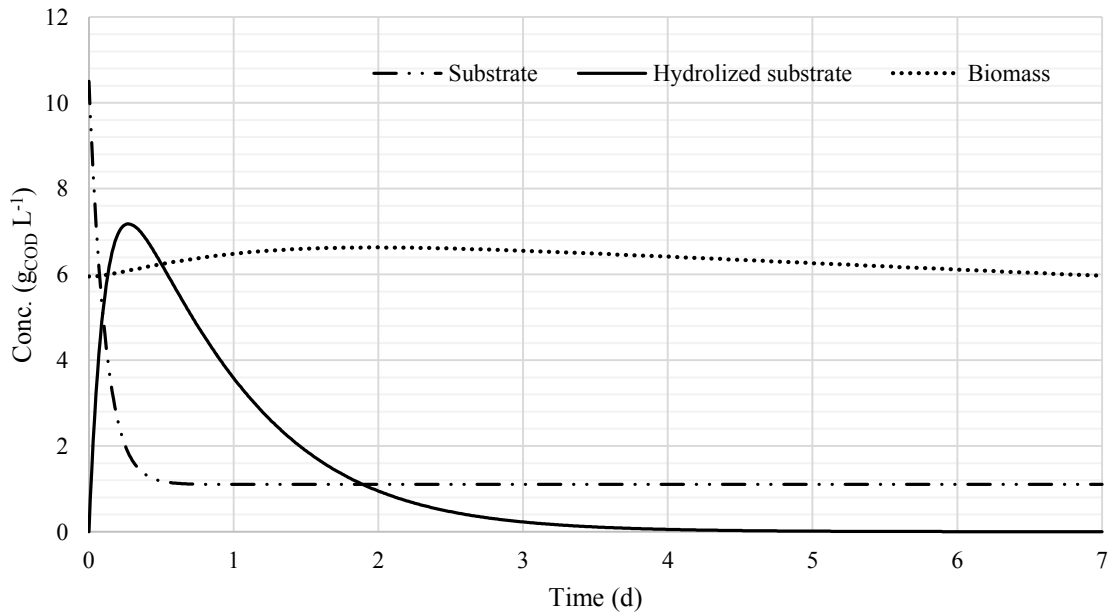


Figure 25. Mashed potatoes: temporal profiles of simulated initial substrate, hydrolyzed substrate and biomass concentration.

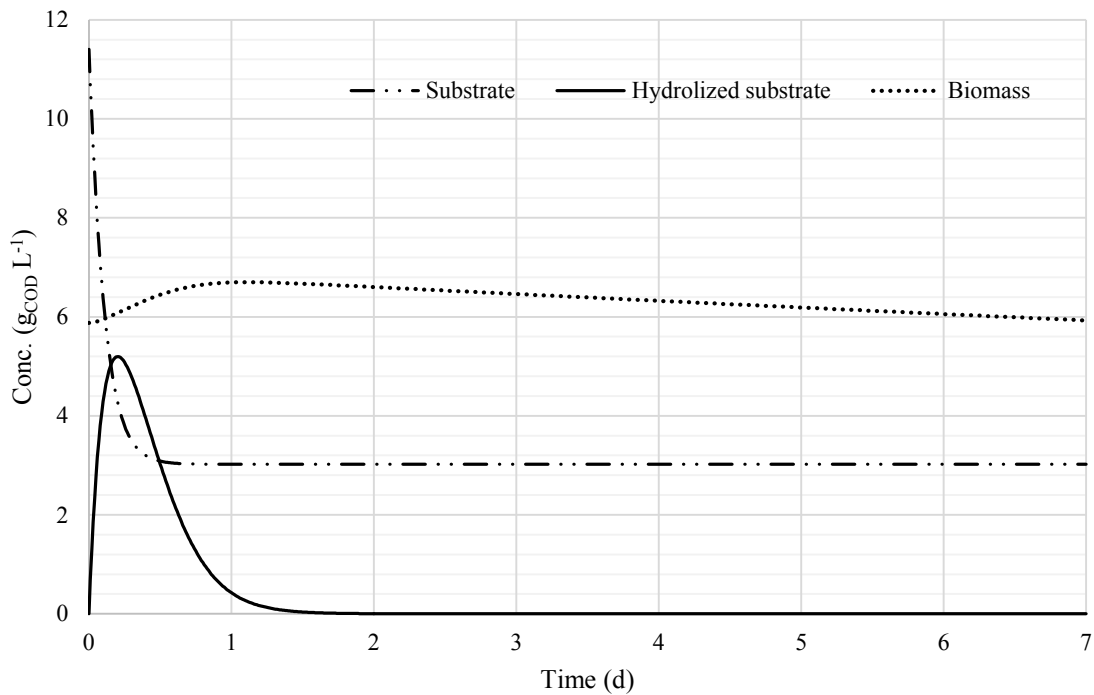


Figure 26. Potato peels: temporal profiles of simulated initial substrate, hydrolysed substrate and biomass concentration.

Comparable values of the kinetic parameters were not found in literature. The general trend in studies about hydrogen production by dark fermentation, especially with particulate substrates, is to use the Gompertz equation (or similar) to describe the hydrogen generation and a Monod-type model just to simulate the dependence of H₂ production on substrate concentration. An example of this approach was reported by Lee et al. (2008) utilizing starch as feedstock. The estimated half saturation Monod constant was 16.28 g_{COD} L⁻¹ (Lee et al. 2008) which is similar to the K_s values reported in Table 4-4.

The initial active biomass concentration estimated by the model in the two test is almost the same. This result was expected since the seed sludge pre-treated and inoculated in the test vessels was the same, at the same concentration. Moreover, the two tests were carried out simultaneously.

The fraction of biodegradable substrate calibrated by the model reflects the composition of the feedstock; 90% of the initial concentration of mashed potatoes and 70% of potato peels expressed as COD are degraded under anaerobic fermentative conditions. The overall lower degradability of the peels is due to the higher content of structural carbohydrates as cellulose, pectin and lignin. Cellulose is less easily degradable than starch and pectin and lignin are not degraded in the tested conditions.

Starch is a carbohydrate consisting of a large number of glucose units joined by glycosidic bonds. It is easily hydrolyzed as can be seen from the values of k_{hyd} in Table 4-4. The standard errors of these parameters are high as was observed and discussed previously for the calibration on sucrose. Mashed potatoes have a higher content of starch (i.e. of glucose), in fact the half saturation constant is similar to the one reported in Table 4-1 where glucose was the substrate.

Generally, the kinetic parameters estimated for the tests using potato-processing wastes are quite similar to the glucose ones. As said before, this is due to the high starch content, which is a polymer of glucose and to the use of the same inoculum.

Figure 22 shows the two curves of cumulative hydrogen production from the BHP test simulations of mashed potatoes and potato peels.

The initial exponential production phase is similar for the two substrates but while from potato peels the hydrogen production almost stops at day one reaching a plate, the production from mashed potatoes goes further, decreasing gently the sloping until day three. The higher hydrogen production from the latter substrate is correlated to the higher degree of initial COD utilization. Figure 25 and Figure 26 report the temporal trends of the substrate concentrations. Potato peels are hydrolyzed just partially, about $3 \text{ g}_{COD} \text{ L}^{-1}$ remain unutilized. Moreover, the curve representing the temporal trend of the hydrolyzed substrate of mashed potatoes has a longer tail, reflecting the hydrogen and VFAs generation trends over time.

Biomass concentration in both the simulations is almost constant over time, with a slight increase during the first days, when exponential growth takes place.

The fraction of solubilized substrate, used for the bacterial catabolism and turned into VFAs, is slightly higher for the mashed potatoes. The value of r_{acid} is almost the same of the one estimated for glucose fermentation.

The parameters $n_{1,mo}$ and $n_{2,mo}$ calibrated on potato peels are slightly higher than the mashed potatoes ones, while for the hydrogen yields $h_{2,ac}$ and $h_{2,bu}$, it is the other way around. Therefore, from the fermentation of potatoes peels, a relative higher production of acetic and propionic acid (and consequent lower generation of butyric acid) comes together with a lower gain of hydrogen per mole of acid produced.

The relative increase of acetic acid production in potato peels fermentation can be recognize comparing Figure 23 and Figure 24. The curves representing butyric and acetic acid concentration are closer to each other in the simulation using potato peels as feedstock.

The decay rate constant estimated in both the cases has a standard deviation even higher than the value itself. The variation of this parameter, at least in a reasonable range of values, seems to have little effect on the fitting of measured values from batch tests with short duration as the BHP tests.

Figure 27 and Figure 28 show how the COD of the initial substrate fractionate. The left pie charts represent the unused and the degraded fractions of the feedstock. The charts on the right highlight how the hydrolysed part is subdivided respect to the overall COD.

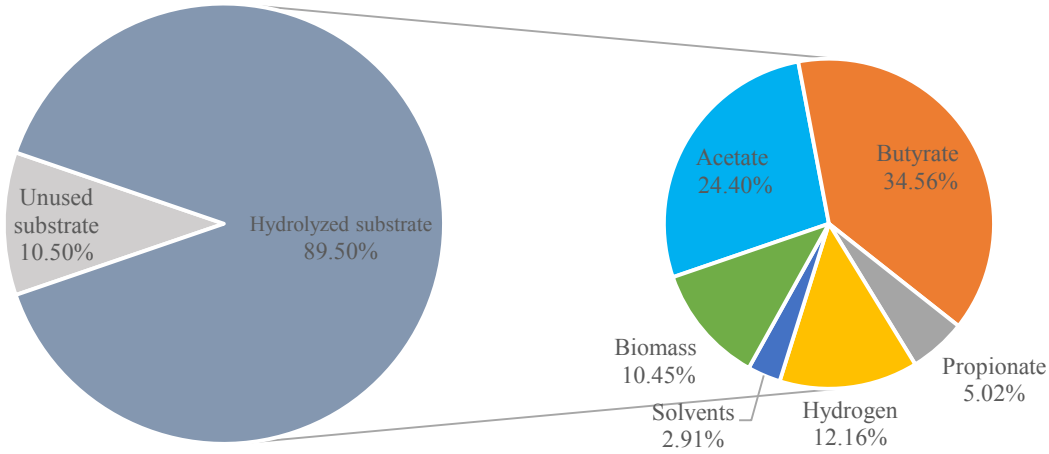


Figure 27. Mashed potatoes: substrate COD fate.

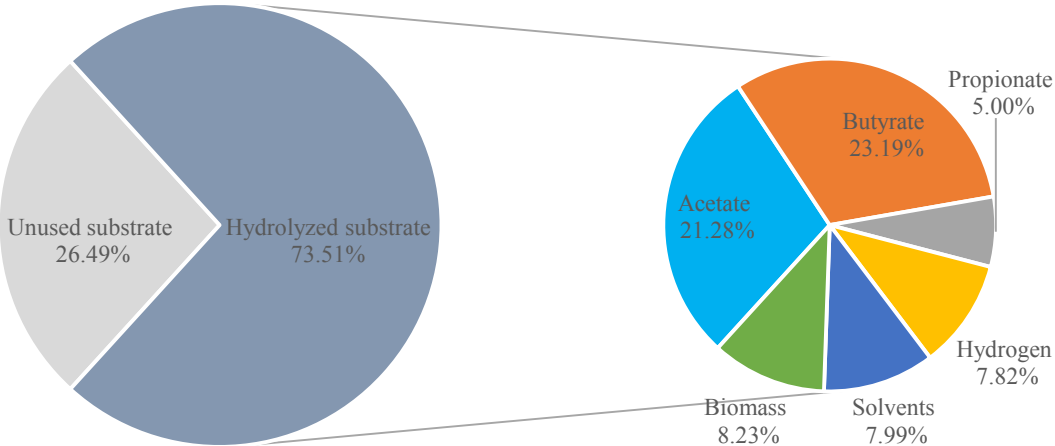


Figure 28. Potato peels: substrate COD fate.

From the two figures, it can be recognize the higher amount of substrate utilized and the higher efficiency of the acidification pathway when mashed potatoes are utilized as feedstock. This is even more marked if the fractions of metabolites are scaled on the degradable part of the substrate. The hydrogen generation yield on the degraded COD estimated by the model is 0.12 $\text{g}_{\text{COD}} \text{g}_{\text{COD}}^{-1}$ on mashed potatoes and 0.11 $\text{g}_{\text{COD}} \text{g}_{\text{COD}}^{-1}$ on potato peels. The yields are similar to those obtained from the calibration on glucose and sucrose and are comparable with literature results of batch tests utilizing starch as substrate (Wang and Wan, 2009).

4.2.4 Model calibration on wheat bran and durum wheat bran BHP batch tests

Wheat bran of *Triticum aestivum* for the production of the common wheat and wheat bran of *Triticum durum* for the production of the durum wheat of the typical Italian pasta were utilized by Giordano et al. (2011) as feedstock for BHP batch tests. Wheat bran's biochemical composition shows that the main component of the dry weight is hemicellulose (30%). Cellulose constitute around 10% of the dry weight while almost all the rest is lignin and pectin (Phyllis2 - ECN Phyllis classification). Hemicellulose is a heteropolymer composed by hexose and pentose saccharides. While cellulose is crystalline, strong, and resistant to hydrolysis, hemicellulose has a random, amorphous structure with little strength. It is hydrolyzed easier than cellulose.

The model parameters were calibrated to fit the hydrogen production and the VFAs generation. The starting values for the parameters estimation were those obtained from the calibration of the waste coming from the potato processing. However, they are expect to change given the different biochemical composition of the feedstock. Table 4-5 shows the calibrated parameters with standard errors for the two BHP tests.

Table 4-5. Model parameters for batch test with wheat bran industrial food wastes.

Source	Best-fit	Best-fit
Substrate	Wheat bran	Durum wheat bran
Initial substrate (g _{COD} L ⁻¹)	23.90	26.60
Seed sludge(g _{COD} L ⁻¹)	56.80	56.80
Initial active biomass (g _{COD} L ⁻¹)	8 ± 0.35	8.1 ± 0.95
K _s (g _{COD} L ⁻¹)	9.1 ± 0.53	14 ± 2.8
f _{bio}	0.41 ± 0.01	0.51 ± 0.01
k _{hyd} (d ⁻¹)	98.6 ± 21	97.8 ± 53.1
km (d ⁻¹)	4.5 ± 0.18	4.8 ± 0.5
μ _{max} (g _{CODs} g _{CODX} ⁻¹ d ⁻¹)	0.36 ± 0.1	0.34 ± 0.13
k _d (d ⁻¹)	0.017 ± 0.11	0.012 ± 0.22
nue _{1_mo}	0.43 ± 0.01	0.45 ± 0.03
nue _{2_mo}	0.12 ± 0.01	0.07 ± 0.03
h _{2_ac}	0.1 ± 0.01	0.1 ± 0.01
h _{2_bu}	0.11 ± 0.01	0.14 ± 0.01
r _{acid}	0.87 ± 0.015	0.88 ± 0.04
Y _B (g _{CODX} g _{CODs} ⁻¹)	0.08 ± 0.02	0.07 ± 0.02

The estimated parameters have been used to perform a simulation of the two batch systems starting from similar initial COD concentration, 23.9 g_{COD}L⁻¹ of wheat bran and 26.6 g_{COD} L⁻¹ of durum wheat bran. The following figures show the simulations of cumulative hydrogen production, VFAs concentration build up and substrate utilization.

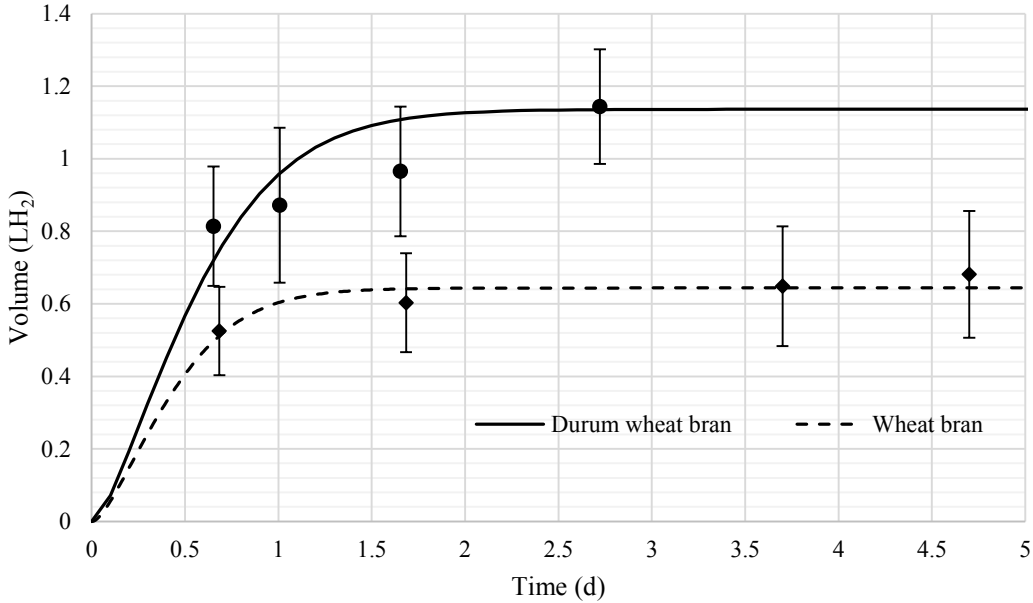


Figure 29. Measured vs predicted hydrogen generation profiles. Symbols represent measured values with the error bars showing the standard deviation. Symbols: Wheat bran (●) and durum wheat bran (◆).

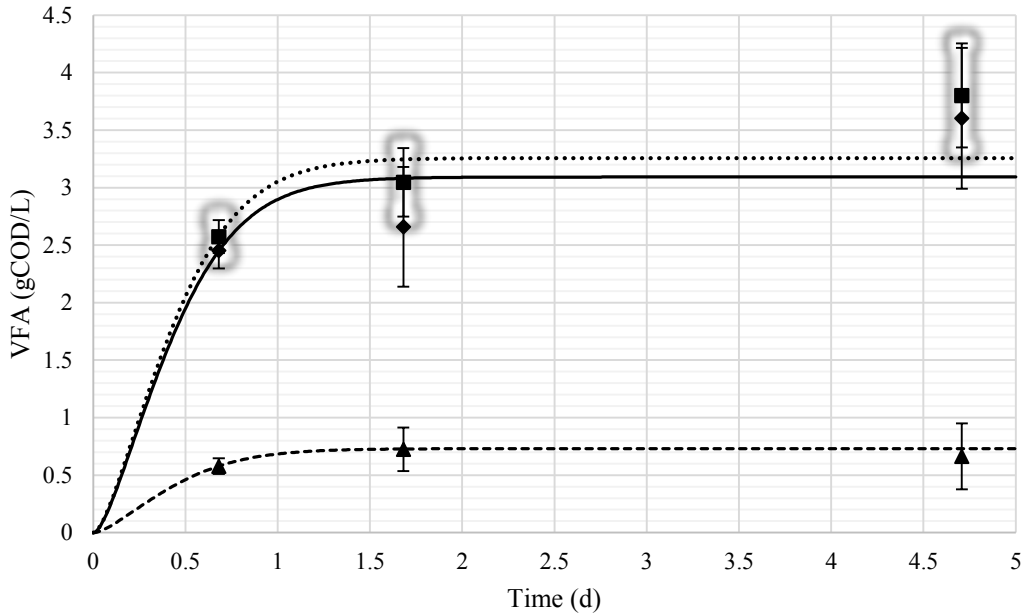


Figure 30. Wheat bran: measured vs predicted VFAs profiles. Symbols represent measured values with the error bars showing the standard deviation. Symbols: acetic (■) butyric (◆) and propionic (▲) acid.

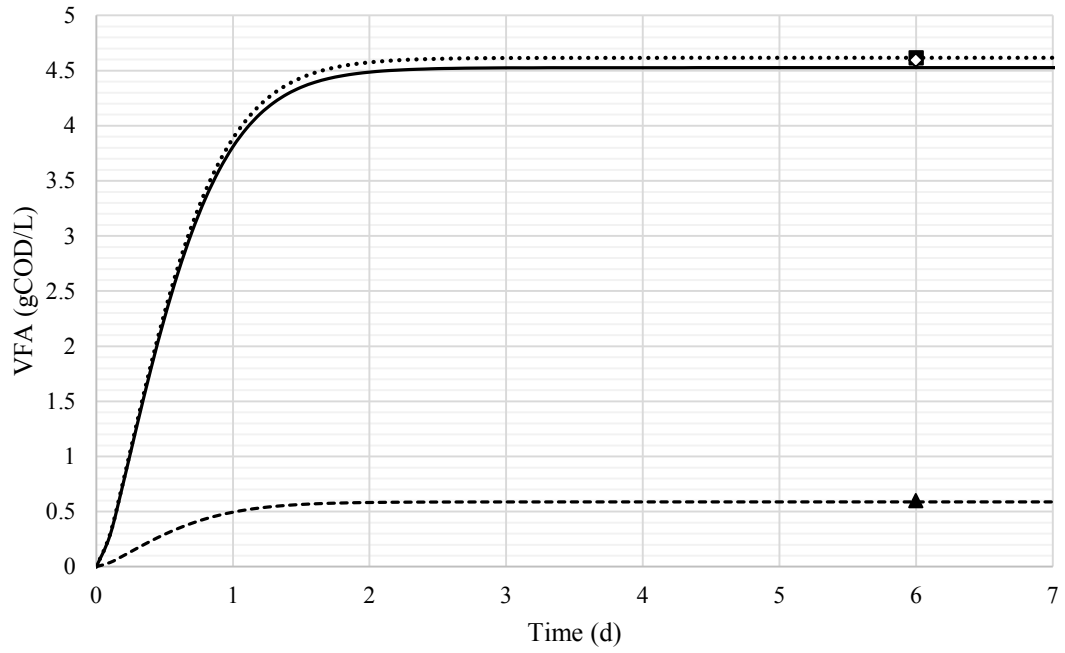


Figure 31. Durum wheat bran: measured vs predicted VFAs profiles. Symbols represent measured values with the error bars showing the standard deviation. Symbols: acetic (■) butyric (◇) and propionic (▲) acid.

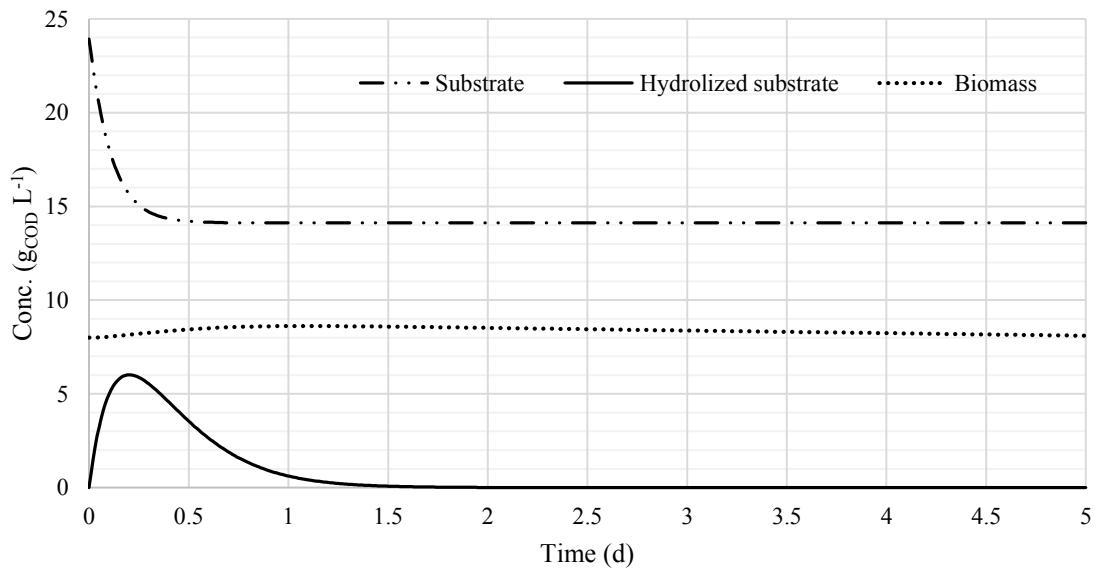


Figure 32. Wheat bran: temporal profiles of simulated initial substrate, hydrolysed substrate and biomass concentration.

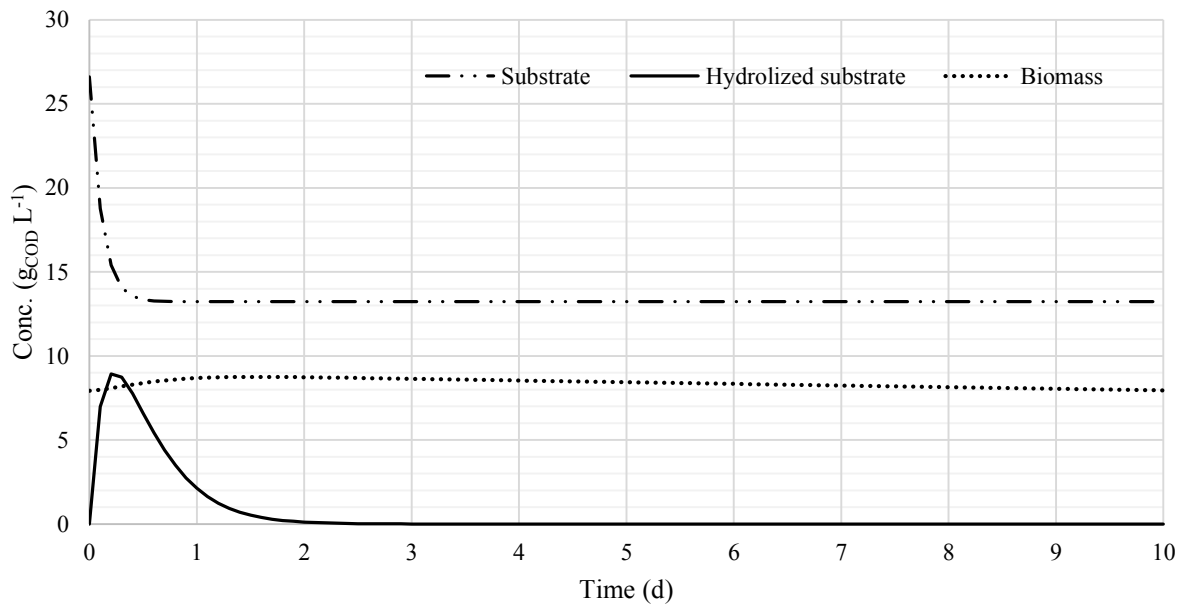


Figure 33. Durum wheat bran: temporal profiles of simulated initial substrate, hydrolysed substrate and biomass concentration.

Comparable values of the kinetic parameters were not found in literature. Most of the studies using complex biomasses as substrates for dark fermentation focus on the hydrogen yields rather than on modelling the process. The evolution of hydrogen production over time in batch conditions is often fitted using the Gompertz equation, which describes the time evolution of hydrogen generation using three parameters, the H₂ production potential, the maximum H₂ production rate and the lag time. Parameters of little value from the biochemical point of view.

The initial active biomass concentration estimated by the model in the two test is almost the same. The seed sludge pretreated and inoculated in the test vessels was in fact the same, at the same concentration. It seems that the model is reasonably able to estimate this parameter.

The fraction of biodegradable COD calibrated by the model reflects the composition of the substrates; 40% of the initial concentration of wheat bran and 50% of durum wheat bran expressed as COD are degraded under anaerobic fermentative conditions. The two wheat brans come from different industrial processes. It is not surprising a slightly variability in the biodegradable fraction. The component of wheat bran that is most probably degraded is hemicellulose. It is easily hydrolysable and explains the values of k_{hyd} in Table 4-5. The standard errors of these parameters are high as was observed in the previous simulations with sucrose and potatoes. The kinetic parameters estimated by the model for the two type of wheat bran are similar with each other. Moreover, when compared with the parameters coming from the calibration on potato residues, it can be observed that the parameters describing the bacteria kinetics are almost the same. What is

changing are the values of the constants defining the microorganism metabolism (i.e. $n_{1,mo}$, $n_{2,mo}$, $h_{2,ac}$, $h_{2,bu}$ and Y_{mo}). The fermentative bacteria are growing slower on wheat bran, using less substrate for the anabolism. It is also visible from Figure 32 and Figure 33 where can be see that the concentration of biomass is almost constant during the simulation. The parameters describing the reaction pathways and the hydrogen yields suggest that, when fermenting wheat bran, the biomass is generating more acetic acid than during the degradation of potato residues but with lower hydrogen production. From the acetic acid generation pathway are obtained 1.2 moles of H_2 per mole of glucose equivalent, almost a half of the yield from the generation of the same acid with mashed potatoes as substrates. The yield from butyric acid generation is slightly lower as well.

An explanation could be found in the different biochemical composition of wheat bran and potato residues. As was previously reported, the degradable part of wheat bran is mainly hemicellulose, while potatoes are rich in starch. Hemicellulose contain both hexoses and pentoses while starch is a polymer of glucose. Hence the differences in fermentation efficiencies.

Figure 30 and Figure 31 report the VFAs concentration over time. The acetic and butyric acid concentration, expressed in $g_{COD} L^{-1}$, is closed in both the tests with wheat bran.

The different BHP of the two substrates observed in Figure 29 is mainly due to the different degree of hydrolysis and initial substrate COD (Figure 32, Figure 33). Both were higher for durum wheat bran, which showed a higher hydrogen generation.

The fate of the substrate COD is reported in Figure 34 for wheat bran and Figure 35 for durum wheat bran. The left pie charts represent the unused and the degraded fractions of the feedstock. The chart on the right highlights how the hydrolysed part is subdivided respect to the overall COD.

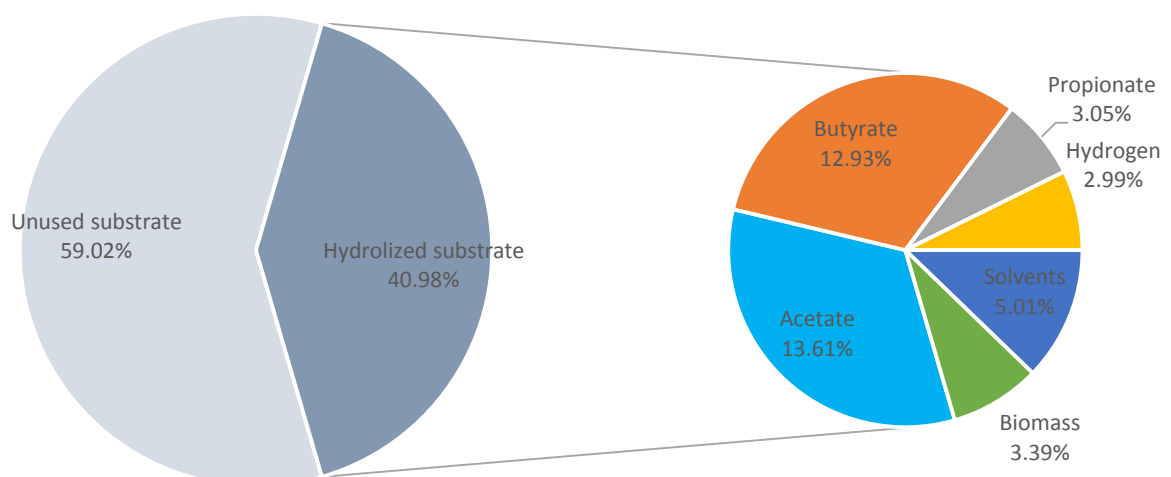


Figure 34. Wheat bran: substrate COD fate.

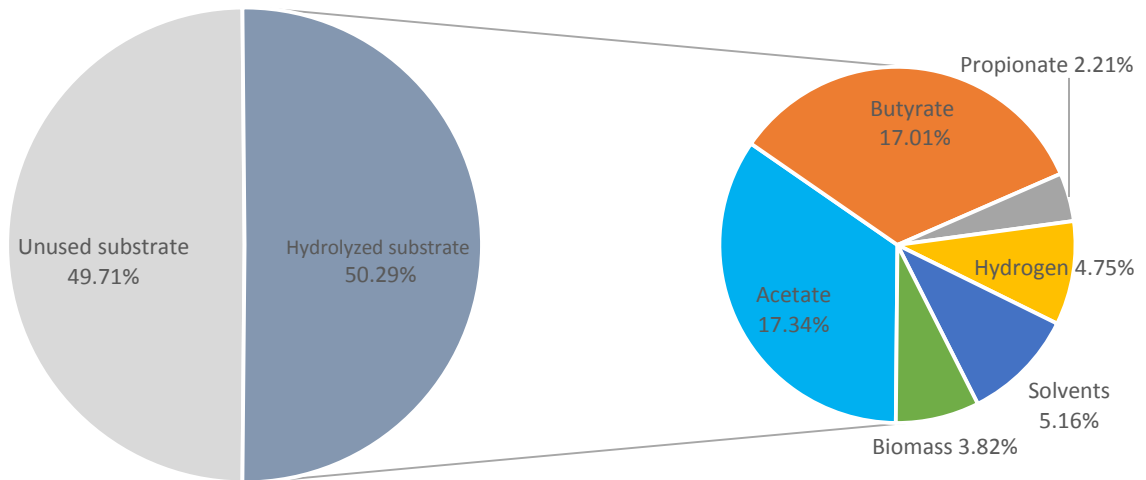


Figure 35. Durum wheat bran: substrate COD fate.

From the two figures can be recognize once again the higher amount of substrate degraded when durum wheat bran is utilized as feedstock. Probably, the different industrial process in which this kind of wheat is involved improves the accessibility to the carbohydrates.

The hydrogen generation yield estimated by the model on the degraded COD is $0.07 \text{ g}_{\text{COD}} \text{ g}_{\text{COD}}^{-1}$ on wheat bran and $0.1 \text{ g}_{\text{COD}} \text{ g}_{\text{COD}}^{-1}$ on durum wheat bran.

The higher H_2 yield on durum wheat bran derive from the small difference of the metabolic parameters estimated (Table 4-5), resulting in a more efficient acidification.

4.2.5 Model calibration on sucrose CSTR continuous test

The model parameters were finally estimated using the experimental data obtained from a CSTR fed on sucrose. The structure of the model was unvaried. To switch from batch to continuous conditions, a dynamic input was added to the reactor compartment of AQUASIM (see paragraph 3.1).

The model parameters were calibrated on experimental data of the hydrogen and VFAs production, and of the substrate consumption. The starting values for the parameters estimation were those obtained from the simulations of the batch tests with sucrose. However, they are expect to change given the different operating conditions and duration of the test. Table 4-6 reports the calibrated parameters with standard errors for the batch test with higher F/M ratio of sucrose, the calibrated parameters for the CSTR test and comparable results retrieved from literature.

Table 4-6. Model parameters for CSTR dark fermentation test.

Source	Best-fit	Best-fit	Literature
Reactor type	Batch	CSTR	CSTR
Substrate	Sucrose	Sucrose	Sucrose
Initial substrate (gCODL^{-1})	9.32	25.00	-
Seed sludge (gCODL^{-1})	5.91	9.50	-
Initial active biomass (gCODL^{-1})	2.34 ± 0.07	4.5 ± 0.17	-
K_s (gCODL^{-1})	13.2 ± 0.72	0.09 ± 0.08	0.07 [1]
f_{bio}	1.00	1.00	-
k_{hyd} (d^{-1})	150 ± 20	250 ± 100	-
k_m (d^{-1})	9.79 ± 0.25	6.87 ± 0.05	-
μ_{max} ($\text{gCODs gCODX}^{-1} \text{d}^{-1}$)	0.98 ± 0.16	0.48 ± 0.01	4 [1]
k_d (d^{-1})	0.06 ± 0.05	0.33 ± 0.005	-
nue_{1_mo}	0.4 ± 0.02	0.58 ± 0.05	-
nue_{2_mo}	0.16 ± 0.01	0.01 ± 0.002	-
h_{2_ac}	0.28 ± 0.004	0.32 ± 0.01	-
h_{2_bu}	0.16 ± 0.006	0.16 ± 0.01	-
r_{acid}	0.75 ± 0.007	0.25 ± 0.03	-
Y_B (gCODX gCODs^{-1})	0.1 ± 0.013	0.07 ± 0.001	0.12 [1]

[1] Chen et al., 2001

The estimated parameters have been used to perform a simulation of the continuous system starting from an initial COD concentration of $25 \text{ g}_{\text{COD}}\text{L}^{-1}$ of sucrose and a mean organic loading rate (OLR) of $12.5 \text{ g}_{\text{COD}}\text{L}^{-1} \text{ d}^{-1}$, which was varied (halved) within the trial. The following figures show the simulations of cumulative hydrogen production, VFAs concentration build up, substrate utilization and volatile suspended solids (VSS) concentration.

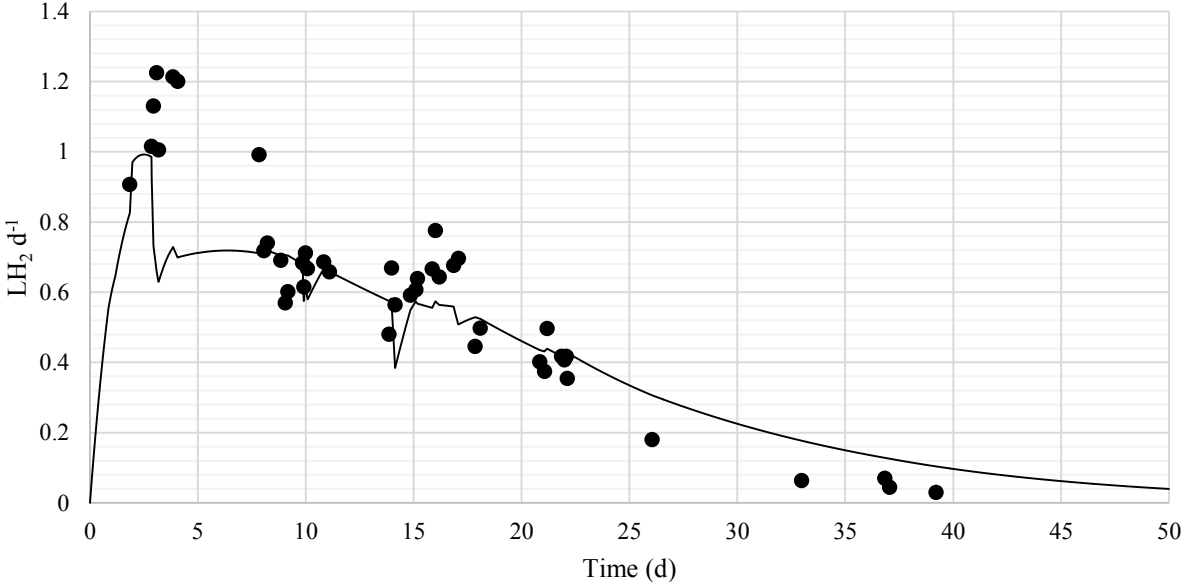


Figure 36. Measured vs predicted hydrogen generation rate profile. Symbols represent measured values (●).

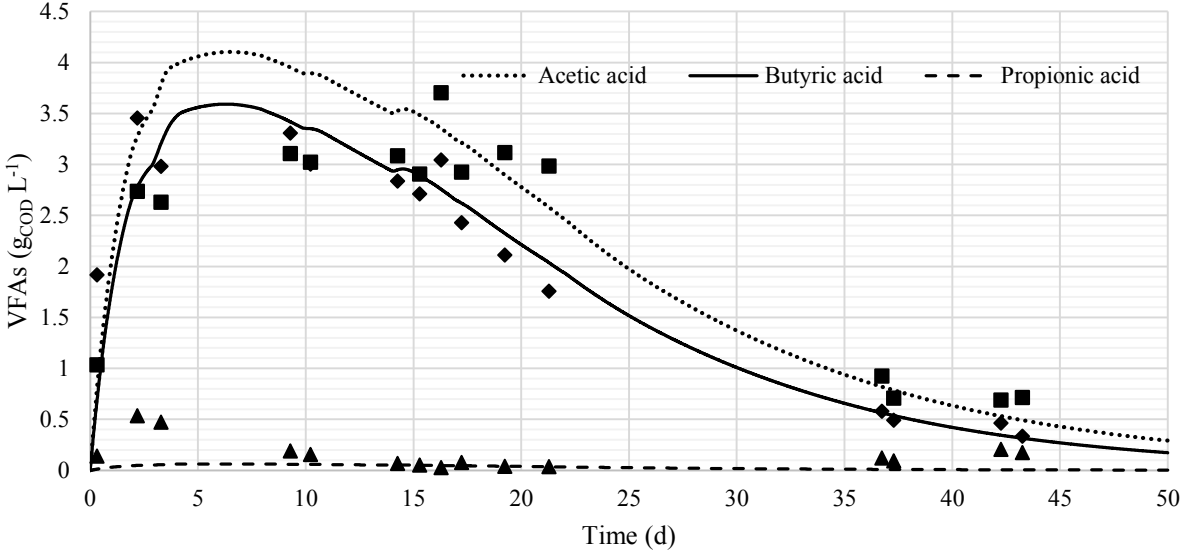


Figure 37. Measured vs predicted VFAs profiles. Symbols represent measured values while the lines show the simulations. Symbols: acetic (■) butyric (◆) and propionic (▲) acid.

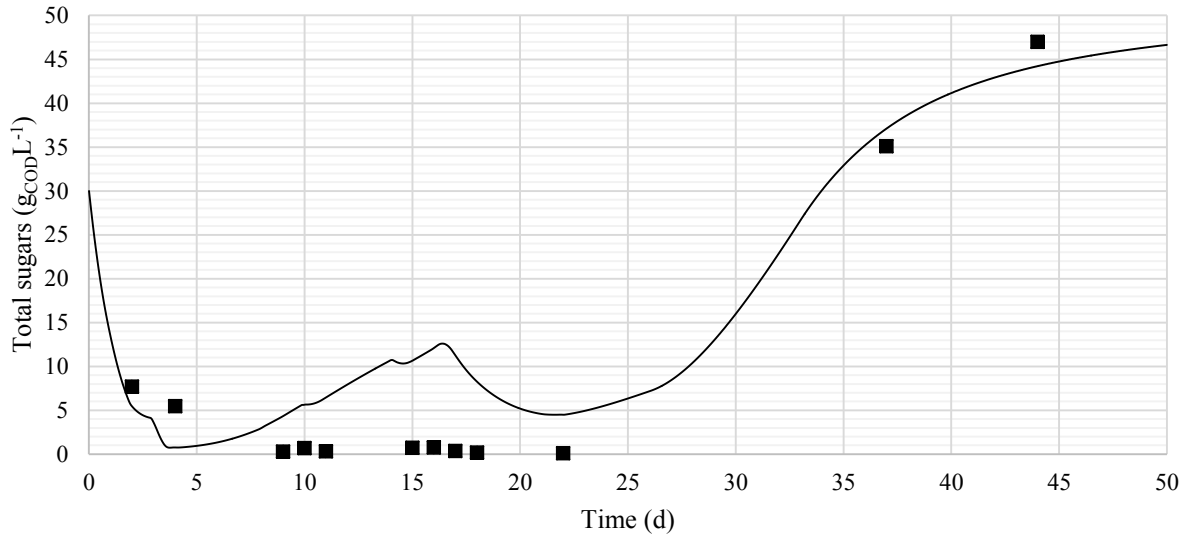


Figure 38. Measured vs predicted total sugars. Symbols represent measured values (■).

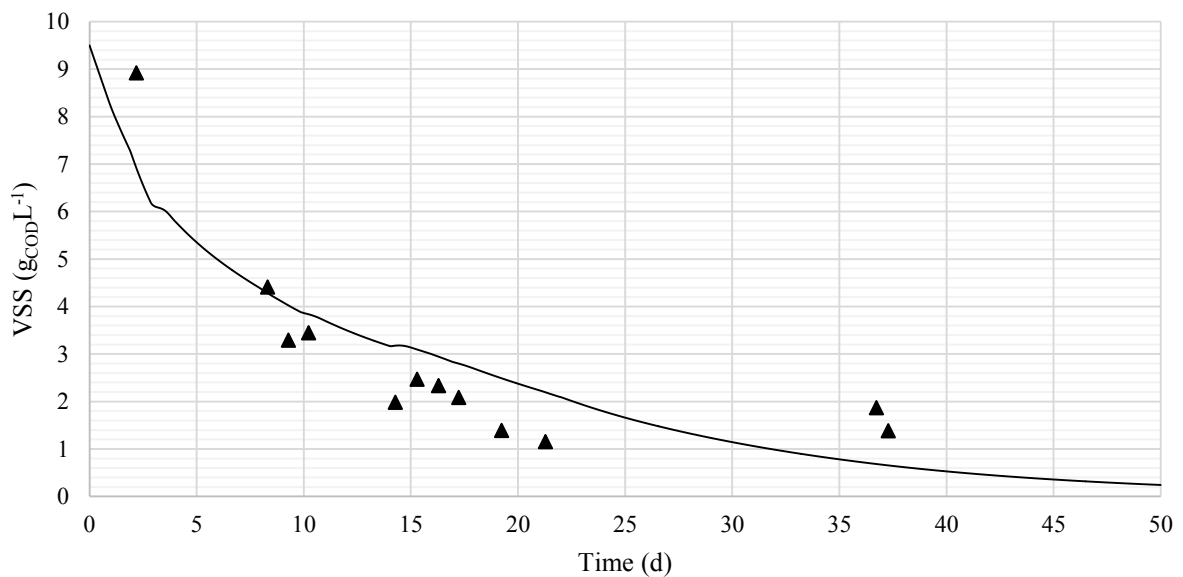


Figure 39. Measured vs predicted VSS concentration. Symbols represent measured values (▲).

The model has estimated the fraction of initial active biomass.

The estimated half saturation constant is similar to the one find out by Chen. et al. (2001) using a CSTR fed with sucrose. The value of K_s estimated in batch conditions, is, on the contrary, one order of magnitude higher than that obtained under continuous conditions. The difference is probably due to the absence of mixing in the batch test, which leads to a lower contact of the biomass and therefore lower substrate availability. In addition, the same hypothesis could also explain the higher value of the hydrolytic constant obtained in continuous conditions.

The values of the calibrated maximum uptake rate and biomass yield result in a maximum specific growth rate halved with respect to the batch test and one order of magnitude lower than the literature data. This parameter is sensible to temperature and pH and it is strictly related to the specific microorganism of the fermentation process. In this particular case however, μ_{\max} is accompanied by a high decay rate. The HPB probably suffered a lack of important micronutrients for their development. This consideration is supported by the low fraction of acidogenesis (r_{acid}); in fact, only the 25% of the degradable substrate has been utilized following the metabolic pathways leading to hydrogen generation. It is possible that during the experimental trial, because of the depletion in particular micronutrients, the microbial population and/or the metabolic paths have changed.

The hydrogen yield on the consumed sucrose estimated by the model is $0.06 \text{ gCODgCOD}^{-1}$, which corresponds to the average yield calculated from the experimental data (Table 4-7).

Table 4-7. Yields of hydrogen generation on sucrose calculated from the experimental data.

Time (d)	Hydrogen yield on sucrose		
	(mL g ⁻¹)	(mol mol ⁻¹)	(gCODgCOD ⁻¹)
1.00	173.38	2.47	0.10
3.00	166.52	2.37	0.10
8.00	97.22	1.38	0.06
9.00	84.84	1.21	0.05
9.98	100.91	1.44	0.06
14.00	86.91	1.24	0.05
15.01	90.25	1.28	0.05
16.00	171.16	2.44	0.10
17.00	105.40	1.50	0.06
21.00	95.99	1.37	0.06
36.21	22.41	0.32	0.01
Average	108.64	1.55	0.06

The estimated metabolic parameters in Table 4-6 (i.e. $n_{1,mo}$, $n_{2,mo}$, $h_{2,ac}$ and $h_{2,bu}$) show a high yield of hydrogen per mole of sugar turned into VFA and a favoured acetic and butyric acid formation (Figure 30). However, HPB probably prevailed only at the beginning of the experiment leaving then the place to other fermentative bacteria or changing metabolic pathways.

The high values of $h_{2,ac}$ and $h_{2,bu}$ lead to the assumption that no homoacetogenesis occurred during the experimental trial but probably bio-reactions leading to lactate or ethanol production took place.

The simulated hydrogen generation (Figure 29) underestimates the measured volume in the first half of the trial while is slightly overestimating it in the second half. A change in the microbial diversity could explain this behaviour together with an increased hydrogen partial pressure in the mixed liquor.

The fermentative biomass was not able to grow fast enough to be retained in the reactor because of the high decay rate. Figure 39 shows the VSS concentration over time. The concentration rapidly decrease because almost a half of the VSS was biomass inactivated with the heat pre-treatment, thus was washed out.

The substrate concentration in the reactor, after a sharp decrease in the first days, started to increase from day 25 until reaching the same concentration of the feed (Figure 38). On day 16 the sucrose concentration in the feed was halved for a week. This change in the load is visible in Figure 38 and explained the isolated high hydrogen yield in Table 4-7.

5 CONCLUSIONS

This study aimed to develop a mathematical model to describe the biochemical hydrogen production from various carbohydrate-rich substrates by dark fermentation. Attention was paid to the simulation of H₂, VFAs and substrates evolution under batch and continuous conditions. The developed model was calibrated on experimental data obtained by bench-scale experiments and on data from literature references. In addition, a sensitivity analysis was applied to help the calibration procedure.

The model was capable to reasonably describe the experimental data and the biochemical reactions under both batch and continuous conditions.

The calibrated coefficients are consistent with the seed sludge utilised and the composition of the feedstock, leading to worthy estimations of the fraction of biomass selected with the heat-pre-treatment and of the fraction of degradable substrate under the tested conditions.

The metabolic parameters estimated on the BHP batch tests on sucrose showed that the hydrogen yields on consumed sugar increase at increasing initial substrate concentration.

Among the food industry wastes considered, refuses from the production of mash potatoes and from the steam-peeling potato processing showed to be the most suitable substrates for hydrogen production by dark fermentation with a biodegradable fraction of 90% and 75% respectively. Only a half of the initial COD of wheat brans was instead utilised by the fermentative biomass. Moreover, the hydrogen yields on mashed potatoes are similar to the values estimated for glucose and are higher than the yields on the other substrates.

The maximum specific uptake rate and the degree of acidogenesis in batch conditions were also found to be consistent with the seed sludge utilised. When anaerobic granular sludge was used the maximum uptake rate ranged between 4.15 and 4.8 d⁻¹ while r_{acid} , which represents the fraction of hydrolysed COD metabolized through acidogenesis pathways, was comprised between 96% and 84%. Biomass decay showed to be the less identifiable parameter in short-term batch tests while it presented a reasonable standard error when the continuous configuration was simulated. The estimated half saturation constant in continuous condition was 0.09 g_{COD} L⁻¹, one order of magnitude lower than in batch tests. In addition, r_{acid} and the decay rate (k_d) changed dramatically when switching from batch to continuous configuration. When the CSTR was simulated, the estimated r_{acid} was 25% and k_d was 0.33 d⁻¹, highlighting the importance of specific operating conditions.

The kinetic and metabolic constants obtained from this study are comparable with literature findings and can be used to support the design of hydrogen producing bioprocesses with different reactor configuration and substrates.

The evaluation of the suitability of different feedstock for hydrogen production is important for future industrial-scale application. The model, in fact, enabling the comparison of yields and microbial efficiencies in fermenting different substrates, could support the design of the process scale-up. Moreover, the capacity of the model for predicting end-products could also help the design of downstream processes.

The model proposed in this study could represent a powerful tool for simulating bio-hydrogen production, substrate degradation and metabolites generation as a fair compromise between simplicity of application and mechanistic description of the dark fermentation process.

6 REFERENCES

- Aceves-Lara, C.-A., Latrille, E., Bernet, N., Buffière, P., Steyer, J.-P., 2008. A pseudo-stoichiometric dynamic model of anaerobic hydrogen production from molasses. *Water Res.* 42, 2539–2550. doi:10.1016/j.watres.2008.02.018
- Adessi, A., Philippis, R.D., 2012. Hydrogen Production: Photofermentation, in: Hallenbeck, P.C. (Ed.), *Microbial Technologies in Advanced Biofuels Production*. Springer US, pp. 53–75.
- Alibardi, L., Cossu, R., 2015. Composition variability of the organic fraction of municipal solid waste and effects on hydrogen and methane production potentials. *Waste Manag.* 36, 147–155. doi:10.1016/j.wasman.2014.11.019
- American Public Health Association., Eaton, A.D., American Water Works Association., Water Environment Federation., 2005. *Standard methods for the examination of water and wastewater*. APHA-AWWA-WEF, Washington, D.C.
- Antonopoulou, G., Gavala, H.N., Skiadas, I.V., Lyberatos, G., 2012. Modeling of fermentative hydrogen production from sweet sorghum extract based on modified ADM1. *Int. J. Hydrog. Energy* 37, 191–208. doi:10.1016/j.ijhydene.2011.09.081
- Argun, H., Kargi, F., Kapdan, I.K., Oztekin, R., 2008. Biohydrogen production by dark fermentation of wheat powder solution: Effects of C/N and C/P ratio on hydrogen yield and formation rate. *Int. J. Hydrog. Energy* 33, 1813–1819. doi:10.1016/j.ijhydene.2008.01.038
- Arudchelvam, Y., Perinpanayagam, M., Nirmalakhandan, N., 2010. Predicting VFA formation by dark fermentation of particulate substrates. *Bioresour. Technol.* 101, 7492–7499. doi:10.1016/j.biortech.2010.04.045
- Azwar, M.Y., Hussain, M.A., Abdul-Wahab, A.K., 2014. Development of biohydrogen production by photobiological, fermentation and electrochemical processes: A review. *Renew. Sustain. Energy Rev.* 31, 158–173. doi:10.1016/j.rser.2013.11.022
- Batstone, D.J., Keller, J., Angelidaki, I., Kalyuzhnyi, S.V., Pavlostathis, S.G., Rozzi, A., Sanders, W.T.M., Siegrist, H., Vavilin, V.A., 2002. *Anaerobic Digestion Model No.1 (ADM1) [WWW Document]*. URL <http://www.iwapublishing.com/template.cfm?name=isbn1900222787> (accessed 1.27.15).
- Boni, M.R., Scaffoni, S., Tuccinardi, L., 2013. The influence of slaughterhouse waste on fermentative H₂ production from food waste: Preliminary results. *Waste Manag.* 33, 1362–1371. doi:10.1016/j.wasman.2013.02.024
- Chen, C.-Y., L., J.-S., C., 2001. Kinetics of hydrogen production with continuous anaerobic cultures utilizing sucrose as the limiting substrate. *Appl. Microbiol. Biotechnol.* 57, 56–64. doi:10.1007/s002530100747
- Chen, C.-Y., Yang, M.-H., Yeh, K.-L., Liu, C.-H., Chang, J.-S., 2008. Biohydrogen production using sequential two-stage dark and photo fermentation processes. *Int. J. Hydrog. Energy* 33, 4755–4762. doi:10.1016/j.ijhydene.2008.06.055

- Chen, W.-H., Chen, S.-Y., Kumar Khanal, S., Sung, S., 2006. Kinetic study of biological hydrogen production by anaerobic fermentation. *Int. J. Hydrog. Energy* 31, 2170–2178. doi:10.1016/j.ijhydene.2006.02.020
- Chittibabu, G., Nath, K., Das, D., 2006. Feasibility studies on the fermentative hydrogen production by recombinant *Escherichia coli* BL-21. *Process Biochem.* 41, 682–688. doi:10.1016/j.procbio.2005.08.020
- Contreras, E.M., Bertola, N.C., Giannuzzi, L., Zaritzky, N.E., 2002. A modified method to determine biomass concentration as COD in pure cultures and in activated sludge systems. *Water Sa* 28, 463–468.
- Das, D., Veziroğlu, T.N., 2001. Hydrogen production by biological processes: a survey of literature. *Int. J. Hydrog. Energy* 26, 13–28. doi:10.1016/S0360-3199(00)00058-6
- Davila-Vazquez, G., Arriaga, S., Alatraste-Mondragón, F., de León-Rodríguez, A., Rosales-Colunga, L.M., Razo-Flores, E., 2008. Fermentative biohydrogen production: trends and perspectives. *Rev. Environ. Sci. Biotechnol.* 7, 27–45. doi:10.1007/s11157-007-9122-7
- De Gioannis, G., Muntoni, A., Poletini, A., Pomi, R., 2013. A review of dark fermentative hydrogen production from biodegradable municipal waste fractions. *Waste Manag.* 33, 1345–1361. doi:10.1016/j.wasman.2013.02.019
- De Sá, L.R.V., Cammarota, M.C., de Oliveira, T.C., Oliveira, E.M.M., Matos, A., Ferreira-Leitão, V.S., 2013. Pentoses, hexoses and glycerin as substrates for biohydrogen production: An approach for Brazilian biofuel integration. *Int. J. Hydrog. Energy* 38, 2986–2997. doi:10.1016/j.ijhydene.2012.12.103
- Dubois, M., Gilles, K.A., Hamilton, J.K., Rebers, Pa., Smith, F., 1956. Colorimetric method for determination of sugars and related substances. *Anal. Chem.* 28, 350–356.
- Gadhamshetty, V., Arudchelvam, Y., Nirmalakhandan, N., Johnson, D.C., 2010. Modeling dark fermentation for biohydrogen production: ADM1-based model vs. Gompertz model. *Int. J. Hydrog. Energy* 35, 479–490. doi:10.1016/j.ijhydene.2009.11.007
- Giordano, A., Cantù, C., Spagni, A., 2011. Monitoring the biochemical hydrogen and methane potential of the two-stage dark-fermentative process. *Bioresour. Technol.* 102, 4474–4479. doi:10.1016/j.biortech.2010.12.106
- Hallenbeck, P.C., 2011. Microbial paths to renewable hydrogen production. *Biofuels* 2, 285–302. doi:10.4155/bfs.11.6
- Hallenbeck, P.C., 2009. Fermentative hydrogen production: Principles, progress, and prognosis. *Int. J. Hydrog. Energy, IWBT 2008 IWBT 2008* 34, 7379–7389. doi:10.1016/j.ijhydene.2008.12.080
- Hallenbeck, P.C., Abo-Hashesh, M., Ghosh, D., 2012. Strategies for improving biological hydrogen production. *Bioresour. Technol.* 110, 1–9. doi:10.1016/j.biortech.2012.01.103
- Hallenbeck, P.C., Benemann, J.R., 2002. Biological hydrogen production; fundamentals and limiting processes. *Int. J. Hydrog. Energy* 27, 1185–1193.

- Hawkes, F., Hussy, I., Kyazze, G., Dinsdale, R., Hawkes, D., 2007. Continuous dark fermentative hydrogen production by mesophilic microflora: Principles and progress. *Int. J. Hydrog. Energy* 32, 172–184. doi:10.1016/j.ijhydene.2006.08.014
- Kapdan, I.K., Kargi, F., 2006. Bio-hydrogen production from waste materials. *Enzyme Microb. Technol.* 38, 569–582. doi:10.1016/j.enzmictec.2005.09.015
- Lalauette, E., Thammannagowda, S., Mohagheghi, A., Maness, P.-C., Logan, B.E., 2009. Hydrogen production from cellulose in a two-stage process combining fermentation and electrohydrogenesis. *Int. J. Hydrog. Energy* 34, 6201–6210. doi:10.1016/j.ijhydene.2009.05.112
- Lee, K., Hsu, Y., Lo, Y., Lin, P., Lin, C., Chang, J., 2008. Exploring optimal environmental factors for fermentative hydrogen production from starch using mixed anaerobic microflora. *Int. J. Hydrog. Energy* 33, 1565–1572. doi:10.1016/j.ijhydene.2007.10.019
- Lin, C., Wu, S., Chang, J., 2006. Fermentative hydrogen production with a draft tube fluidized bed reactor containing silicone-gel-immobilized anaerobic sludge. *Int. J. Hydrog. Energy* 31, 2200–2210. doi:10.1016/j.ijhydene.2006.05.012
- Lin, P.-Y., Whang, L.-M., Wu, Y.-R., Ren, W.-J., Hsiao, C.-J., Li, S.-L., Chang, J.-S., 2007. Biological hydrogen production of the genus *Clostridium*: Metabolic study and mathematical model simulation. *Int. J. Hydrog. Energy* 32, 1728–1735. doi:10.1016/j.ijhydene.2006.12.009
- Liu, D., Liu, D., Zeng, R.J., Angelidaki, I., 2006. Hydrogen and methane production from household solid waste in the two-stage fermentation process. *Water Res.* 40, 2230–2236. doi:10.1016/j.watres.2006.03.029
- Lo, Y.-C., Chen, W.-M., Hung, C.-H., Chen, S.-D., Chang, J.-S., 2008. Dark H₂ fermentation from sucrose and xylose using H₂-producing indigenous bacteria: Feasibility and kinetic studies. *Water Res.* 42, 827–842. doi:10.1016/j.watres.2007.08.023
- Meher Kotay, S., Das, D., 2008. Biohydrogen as a renewable energy resource—Prospects and potentials. *Int. J. Hydrog. Energy, IWHE* 2006 33, 258–263. doi:10.1016/j.ijhydene.2007.07.031
- Mu, Y., Wang, G., Yu, H.-Q., 2006. Kinetic modeling of batch hydrogen production process by mixed anaerobic cultures. *Bioresour. Technol.* 97, 1302–1307. doi:10.1016/j.biortech.2005.05.014
- Mu, Y., Yu, H.-Q., Wang, G., 2007. A kinetic approach to anaerobic hydrogen-producing process. *Water Res.* 41, 1152–1160. doi:10.1016/j.watres.2006.11.047
- Nath, K., 2008. Kinetics of two-stage fermentation process for the production of hydrogen. *Int. J. Hydrog. Energy* 33, 1195–1203. doi:10.1016/j.ijhydene.2007.12.011
- Nath, K., Das, D., 2011. Modeling and optimization of fermentative hydrogen production. *Bioresour. Technol.* 102, 8569–8581. doi:10.1016/j.biortech.2011.03.108

- Nath, K., Das, D., 2004. Improvement of fermentative hydrogen production: various approaches. *Appl. Microbiol. Biotechnol.* 65. doi:10.1007/s00253-004-1644-0
- Ntaikou, I., Gavala, H.N., Lyberatos, G., 2010. Application of a modified Anaerobic Digestion Model 1 version for fermentative hydrogen production from sweet sorghum extract by *Ruminococcus albus*. *Int. J. Hydrog. Energy* 35, 3423–3432. doi:10.1016/j.ijhydene.2010.01.118
- Ntaikou, I., Gavala, H.N., Lyberatos, G., 2009. Modeling of fermentative hydrogen production from the bacterium *Ruminococcus albus*: Definition of metabolism and kinetics during growth on glucose. *Int. J. Hydrog. Energy* 34, 3697–3709. doi:10.1016/j.ijhydene.2009.02.057
- Oh, S., Logan, B.E., 2005. Hydrogen and electricity production from a food processing wastewater using fermentation and microbial fuel cell technologies. *Water Res.* 39, 4673–4682. doi:10.1016/j.watres.2005.09.019
- Penumathsa, B.K.V., Premier, G.C., Kyazze, G., Dinsdale, R., Guwy, A.J., Esteves, S., Rodríguez, J., 2008. ADM1 can be applied to continuous bio-hydrogen production using a variable stoichiometry approach. *Water Res.* 42, 4379–4385. doi:10.1016/j.watres.2008.07.030
- Phyllis2 - ECN Phyllis classification [WWW Document], n.d. URL <https://www.ecn.nl/phyllis2/Browse/Standard/ECN-Phyllis#potato> (accessed 3.18.15).
- Rasika J. Perera, K., Nirmalakhandan, N., 2011. Modeling fermentative hydrogen production from sucrose supplemented with dairy manure. *Int. J. Hydrog. Energy* 36, 2102–2110. doi:10.1016/j.ijhydene.2010.11.047
- Reichert, P., 1998. AQUASIM 2.0–user manual. Swiss Fed. Inst. Environ. Sci. Technol. Dubendorf Switz.
- Rodríguez, J., Kleerebezem, R., Lema, J.M., van Loosdrecht, M.C.M., 2006. Modeling product formation in anaerobic mixed culture fermentations. *Biotechnol. Bioeng.* 93, 592–606. doi:10.1002/bit.20765
- Sharma, Y., Li, B., 2009. Optimizing hydrogen production from organic wastewater treatment in batch reactors through experimental and kinetic analysis. *Int. J. Hydrog. Energy* 34, 6171–6180. doi:10.1016/j.ijhydene.2009.06.031
- Show, K.-Y., Lee, D.-J., Chang, J.-S., 2011. Bioreactor and process design for biohydrogen production. *Bioresour. Technol., Special Issue : Biofuels-III: Biohydrogen* 102, 8524–8533. doi:10.1016/j.biortech.2011.04.055
- Show, K.Y., Lee, D.J., Tay, J.H., Lin, C.Y., Chang, J.S., 2012. Biohydrogen production: Current perspectives and the way forward. *Int. J. Hydrog. Energy, The 2011 Asian Bio-Hydrogen and Biorefinery Symposium (2011ABBS)* 37, 15616–15631. doi:10.1016/j.ijhydene.2012.04.109
- Van Ginkel, S.W., Logan, B., 2005. Increased biological hydrogen production with reduced organic loading. *Water Res.* 39, 3819–3826. doi:10.1016/j.watres.2005.07.021

- Van Niel, E.W.J., Claassen, P.A.M., Stams, A.J.M., 2003. Substrate and product inhibition of hydrogen production by the extreme thermophile, *Caldicellulosiruptor saccharolyticus*. *Biotechnol. Bioeng.* 81, 255–262. doi:10.1002/bit.10463
- Wang, J., Wan, W., 2009. Factors influencing fermentative hydrogen production: A review. *Int. J. Hydrog. Energy* 34, 799–811. doi:10.1016/j.ijhydene.2008.11.015
- Wang, J., Wan, W., 2008. The effect of substrate concentration on biohydrogen production by using kinetic models. *Sci. China Ser. B Chem.* 51, 1110–1117. doi:10.1007/s11426-008-0104-6
- Wong, Y.M., Wu, T.Y., Juan, J.C., 2014. A review of sustainable hydrogen production using seed sludge via dark fermentation. *Renew. Sustain. Energy Rev.* 34, 471–482. doi:10.1016/j.rser.2014.03.008
- Zheng, H., Zeng, R.J., Angelidaki, I., 2008. Biohydrogen production from glucose in upflow biofilm reactors with plastic carriers under extreme thermophilic conditions (70°C). *Biotechnol. Bioeng.* 100, 1034–1038. doi:10.1002/bit.21826